An overview of the SOLVE-THESEO 2000 campaign

Paul A. Newman[1], Neil R. P. Harris[2], Alberto Adriani[3], Georgios T. Amanatidis[4], James G. Anderson[5], Geir O. Braathen[6], William H. Brune[7], Kenneth S. Carslaw[8], Michael T. Craig[9], Philip E. DeCola[10], Marielle Guirlet[11], Steve R. Hipskind[9], Michael J. Kurylo[10, 12], Harry Küllmann[13], Niels Larsen[14], Gérard Mégie[15], Jean-Pierre Pommereau[16], Lamont R. Poole[17], Mark R. Schoeberl[1], Fred Stroh[18], Owen B. Toon[19], Charles R. Trepte[17], and Michel Van Roozendael[20]

1. NASA's Goddard Space Flight Center, Greenbelt, MD, USA
2. European Ozone Research Coordinating Unit, Cambridge, United Kingdom
3. CNR, Italy
4. EC, Research DG, Brussels, Belgium
5. Harvard University, Cambridge, MA, USA
6. NILU, Kjeller, Norway
7. Pennsylvania State University, University Park, PA, USA
8. University of Leeds, United Kingdom
9. NASA's Ames Research Center, Moffett Field, CA, USA
10. NASA HQ, Washington DC, USA
11. ACRI-ST, Sophia-Antipolis, France
12. NIST, Gaithersburg, MD, USA
13. University of Bremen, Bremen, Germany.
14. Danish Meteorological Institute, Copenhagen, Denmark.
15. Service d'Aéronomie - IPSL, Paris, France
16. CNRS-SA, Verrières le Buisson, France
17. NASA's Langley Research Center, Hampton, VA, USA
18. FZ Jülich, Aachen, Germany
19. University of Colorado, Boulder, CO, USA
20. Belgian Institute for Space and Aeronomy, Brussels, Belgium.

Abstract: Between November 1999 and April 2000, two major field experiments, the SAGE III Ozone Loss and Validation Experiment (SOLVE) and the Third European Stratospheric Experiment on Ozone (THESEO 2000), collaborated to form the largest field campaign yet mounted to study Arctic ozone loss. This international campaign involved more than 500 scientists from over 20 countries spread across the high and mid-latitudes of the northern hemisphere. The main scientific aims of SOLVE-THESEO 2000 were to study (a) the processes leading to ozone loss in the Arctic vortex and (b) the effect on ozone amounts over northern mid-latitudes. The campaign included satellites, heavy lift balloon launches, 6 different aircraft, ground stations, and scores of ozone-sondes. Campaign activities were principally conducted in 3 intensive measurement phases centered on early December 1999, late January 2000, and early March 2000. Observations made during the campaign showed that temperatures were unusually cold in the polar lower stratosphere over the course of the 1999-2000 winter. These cold temperatures resulted in the formation of extensive polar stratospheric clouds (PSCs) across the Arctic. Heterogeneous chemical reactions on the surfaces of the PSC particles produced high levels of reactive chlorine within the polar vortex by early January. This reactive chlorine catalytically destroyed about 60% of the ozone in a layer near 20 km between late-January and mid-March 2000.

1.0 Introduction

Between November 1999 and April 2000, two major field experiments, the NASA-sponsored SAGE III Ozone Loss and Validation Experiment (SOLVE) and the European Commission-led Third European Stratospheric Experiment on Ozone (THESEO 2000), collaborated to form the largest field campaign yet mounted to study Arctic ozone loss. The main scientific aims of SOLVE-THESEO 2000 were to study (a) the processes leading to ozone loss in the Arctic vortex and (b) the effect on ozone amounts over northern mid-latitudes. A further aim was to validate measurements from the third Stratospheric Aerosol and Gas Experiment (SAGE III) instrument. Unfortunately, SAGE III was not launched on schedule and so this goal was not directly achieved. However, measurements from several satellite instruments are being used in conjunction with SOLVE-THESEO 2000 data for scientific and validation studies. SOLVE-THESEO 2000 involved research aircraft, balloons, ozone-sondes, ground-based and satellite instruments, which were augmented by meteorological and chemical models. In all, more than 500 scientists from over 20 countries (the European Union, Canada, Iceland, Japan, Norway, Poland, Russia, Switzerland and the United States of America) were involved. Descriptions of the SOLVE-THESEO 2000 activities and the early findings were published in the SPARC newsletter [Newman, 2000; Harris *et al.*, 2001].

The joint SOLVE-THESEO 2000 campaign represents a new element of cooperation between researchers and agencies from the EU, the USA, and other countries. This cooperation was officially implemented under the 1998 "European Union / United States Science and Technology Cooperation Agreement". The Agreement was crafted to help promote, develop, and facilitate cooperative research and development activities for mutual benefit in virtually all areas of natural sciences and engineering. In this light, the THESEO 2000 Core Group and the SOLVE Management Team recognized that the issues of chemical ozone loss and the expected ozone recovery in a changing atmosphere (containing increased abundances of greenhouse gases) are complex, and that their study would require scientific research activities that are facilitated by international collaboration. Following early discussions, the two planning groups held a joint meeting in November 1999 and decided to join efforts in the close coordination and implementation of the two campaigns. Common data protocols and data dissemination policies, and a joint workshop on the results were also arranged. There were international suites of instruments on aircraft and balloons. The success of this approach is reflected in the number of papers with authors from Europe and the USA.

Arctic ozone loss has been extensively studied since the discovery of the Antarctic ozone hole [Farman *et al.*, 1985]. The simple fact that such a large area of depleted ozone existed immediately raised the question of whether a similar phenomenon could occur over the Arctic, closer to the heavily

populated areas of Asia, Europe and North America. The confirmation that the ozone loss was caused by chlorine and bromine chemistry underlined the importance of the question. As a result a number of large scientific campaigns have investigated ozone loss in the Arctic stratosphere during winter and spring. These include:

- Airborne Arctic Stratospheric Experiment (AASE, 1989)
- European Arctic Stratospheric Ozone Experiment (EASOE, 1991-92)
- Second Airborne Arctic Stratospheric Experiment (AASE 2, 1991-92)
- Second European Stratospheric Arctic and Mid-latitude Experiment (SESAME, 1994-95)
- Photochemistry of Ozone Loss in the Arctic Region In Summer (POLARIS, 1997)
- Third European Stratospheric Experiment on Ozone (THESEO, 1998-99)

There have also been a number of smaller, focused campaigns investigating processes such as the Vortex Ozone Transport Experiment (VOTE, 1996), the Polar Stratospheric Aerosol Experiment (POLSTAR, 1997) and Airborne Polar Experiment (APE-POLECAT, 1997). These campaigns have been complemented by longer-term observations from ground stations (e.g., the stratospheric composition measurements made within the Network for the Detection of Stratospheric Change (NDSC) and the ozone and meteorological observations made within the WMO-GAW network) and by a number of satellite instruments (e.g., TOMS, MLS, HALOE, SAGE, GOME, and POAM). Such continuity of observation is important, since a striking feature of Arctic ozone loss has been its large interannual variability. Multi-year records give the perspective with which to interpret results from individual, intensively studied winters.

The processes which lead to Arctic ozone loss have thus been closely studied and, qualitatively, they are now fairly well understood. During October and November, a westerly circulation of winds develops in the stratosphere as the polar stratosphere cools. This circumpolar vortex is the dominant feature of the stratospheric circulation during the Arctic winter and is the counterpart of the more stable and long-lived Antarctic vortex. During the long periods of darkness at high latitudes in winter, as the Arctic vortex cools radiatively, sufficiently low temperatures (195K or below) can be reached at which polar stratospheric clouds (PSCs) can form. Heterogeneous chemical reactions occur on the surface of the PSC particles. These reactions lead the conversion of relatively inactive chlorine compounds such as HCl and $ClONO_2$ into ClO, and this ClO causes rapid chemical destruction of ozone in the presence of sunlight. This catalytic ozone loss is deactivated by the reaction of ClO with NO_2 to re-form $ClONO_2$. As this ClO gradually reverts back to the inactive forms, the ozone destruction slows down. These processes largely take place in the Arctic vortex. As the vortex circulation breaks down in spring, ozone-depleted air is mixed with mid-latitude air.

Levels of chlorine and bromine in the Arctic are high enough to cause large ozone losses provided the meteorological conditions are cold enough for the formation of PSCs, particularly during late February and March when sunlight returns to the vortex region. There is a large interannual variability in the dynamics and temperature of the Arctic stratosphere, and large ozone losses have occurred in the colder winters but not in the warmer ones. Modeling studies suggest that the changes in climate will cause a further cooling of the stratosphere, which could lead to enhanced PSC formation and a longer-lived Arctic vortex. These mechanisms would increase the frequency of winters with large Arctic ozone losses. An improved understanding of the dynamic, radiative and chemical processes involved is required to increase confidence in model studies of the possible future atmosphere.

The main results of SOLVE-THESEO 2000 are being published in two special sections of JGR [1st vol number; this issue]. In this paper we present an overview of the campaign. In the rest of the introduction, the scientific goals of the campaign are described. In section 2, the full scope of the mission is described with details about the timing and coverage, the platforms (aircraft, balloons, ground-based stations and satellites) and instruments involved, and the meteorological and modeling support activities. A brief outline of the main results to date is given in section 3.

1.1 Scientific Goals

Each element of the chain of processes involved in chemical ozone loss needs to be understood quantitatively if the future evolution of ozone over the Arctic and the northern mid-latitudes is to be accurately assessed. Based on the simple picture given above, the scientific aims can be divided into four main categories:

- Transport and dynamics
- Formation and composition of PSCs
- Improved quantification of the activation and deactivation of halogen oxides
- Empirical and modelled calculations of chemical ozone loss

These more detailed aims are now considered in turn.

1.1.1 Transport and dynamics

Understanding the transport and dynamics of the development and break-up of the Arctic vortex, needed to fully constrain the chemical evolution, requires precise large scale observations over at least one Arctic winter. *In situ* observations of the Arctic stratosphere during the early and mid winter have been relatively sparse. It was important to study this period in detail because the dynamical evolution of the vortex during this period has a major significance in terms of the chemical and dynamical behavior in the January to March period when nearly all the ozone loss takes place. For example, the amount of descent in the vortex resulting from radiative cooling determines the amounts of Cl_y, Br_y and NO_y in spring, while the temperature history determines the extent of PSC formation and, indirectly, the degree of denitrification.

The exchange of air between the polar vortex and the mid-latitudes is also an important factor in the polar ozone budget. Further, the transport of low ozone air from the polar vortex into mid-latitudes can reduce mid-latitude ozone levels. In addition, while mid-latitude air is not easily carried into the polar vortex, occasionally, under disturbed stratospheric weather conditions, mid-latitude air can be entrained into the vortex, significantly changing the chemical composition of the vortex. Small-scale exchange can also provide weak transport across the vortex edge.

1.1.2 Formation and composition of PSCs

PSCs provide the surfaces for the heterogeneous reactions that result in ozone loss, and they also sequester and re-distribute (or remove) nitric acid and water from the stratosphere. The heterogeneous reaction rates on PSCs are known from laboratory measurements but are rather poorly constrained by atmospheric observations, particularly of the chemical composition of the particles. A wide number of questions are still open with respect to the types of PSCs and their composition. These questions were principally addressed during SOLVE-THESEO 2000 by direct measurement and analysis of the chemical and physical composition of PSCs. Information was needed on the temporal evolution of PSCs, in particular the nucleation of these particles and the evolution of their size distributions. Other important questions for PSCs concerned the spatial and horizontal morphologies of the PSC types and size distributions, and their relation to the broad temperature fields. A good understanding of these factors is necessary for broad-scale models to include valid parameterizations for PSC occurrence and the subsequent heterogeneous activation and denitrification process.

1.1.3 Improved quantification of the activation and deactivation of halogen oxides

The chemical depletion of ozone by halogen oxides involves three main areas: the activation processes; the ozone loss cycles; and the deactivation back to the reservoir species. The activation requires the presence of PSCs and so an important question is how the seasonal evolution of the PSCs regulates the activation through the winter? Second, how do the chemical budgets of the nitrogen, chlorine and bromine families evolve over the course of the winter due to repeated activation events? In particular, the impact of synoptic scale and mountain wave mesoscale temperature perturbations has to be considered for an understanding of chlorine activation.

In terms of the ozone loss cycles, the questions mainly relate to understanding and improved quantification of the relative contributions among catalytic loss cycles to the overall ozone loss in the winter to spring period. In particular, what is the importance of ClOOCl in the overall ozone loss and what is the role of Br-containing compounds. Underlying these issues is how the different chemical families interact (under a wide range of conditions) and how this affects the overall chemical ozone loss.

Finally, our current understanding of deactivation (the termination of the halogen catalyzed ozone loss) is that it depends on the reintroduction of NO_2 into the gas phase through the photolysis of nitric acid where it reacts with ClO to form the relatively long-lived $ClONO_2$. The key chemistry questions here thus concerned the rate of production of NO_2 back into the polar stratosphere in spring. A related important issue is how denitrification affects the chlorine deactivation processes and hence ozone loss.

1.1.4 Empirical and modeled calculations of chemical ozone loss

A number of techniques for determining empirical estimates of chemical ozone loss rates in the Arctic vortex have been developed in recent years. Several of these techniques were used during the 1999/2000 winter. It is important to examine the consistency of the empirical estimates with each other, as there has been considerable discussion of apparent inconsistencies between results from different winters.

Comparison of these empirical estimates of ozone loss with the losses calculated by models was another priority for SOLVE-THESEO 2000. Several studies have shown significant disagreements between the modeled and empirical estimates [e.g., Becker *et al.*, 2000; Kilbane-Dawe *et al.*, 2001], and these disagreements limit the confidence that can be placed in predictions of future losses. A

particular puzzle has been the high ozone loss rates observed at the end of January in several years [e.g., Rex *et al.*, 1999]. Thorough comparisons using a range of models are needed to understand better the conditions where these disagreements arise.

2.0 Mission scope

The SOLVE-THESEO 2000 campaign was primarily conducted in 3 phases over the Arctic and mid-latitude region during the winter of 1999-2000. Most activities took place at Kiruna (68°N, 21°E), Sweden or the Swedish Space Corporation (SSC) Esrange facility 40 km from Kiruna. In late 1999, during the first phase, the NASA DC-8 was deployed in Kiruna and two large and two small balloons were launched. Between mid-January and March 2000, in the 2nd and 3rd phases, 7 large balloons, 14 small balloons and 3 long duration balloons carrying scientific payloads were launched successfully from Esrange. Two of the small balloons were launched from the Norwegian station in Andøya. Aircraft measurements in the Arctic region were made on board the NASA ER-2, NASA DC-8, DLR Falcon, the CNRS/INSU ARAT, and the Swiss Air Force Learjet. In addition, the CNRS/INSU Mystère 20 was flown at mid-latitudes. There were simultaneous ground-based activities from the Scandinavian stations (ALOMAR, Kiruna, Ny-Ålesund, Sodankylä, Harestua) throughout the winter, along with other ground measurements from numerous sites across the Arctic. In coordinated activities, the aircraft often flew along upwind and downwind of the balloon flight path. Additional flights of ozone-sondes were conducted at a number of sites across the northern hemisphere [Rex *et al.*, 2001], and ground measurements were made at a number of Arctic and mid-latitude sites.

The TOMS, GOME and POAM satellite instruments also made measurements of sunlit regions of the stratosphere through the winter. Meteorological support was provided by several meteorological organizations, some with representatives in the field (FU-Berlin, US NOAA/NCEP, US Naval Research Lab, NASA/GSFC Data Assimilation Office) to assist daily planning, and others through the provision of data (ECMWF, Meteo-France, SMHI, UKMO and DWD). Modeling and theory support groups were essential for both the pre-mission planning and the daily operational planning.

2.1 Location and Timing

The SOLVE-THESEO 2000 campaign was designed for both extensive spatial coverage and fall-to-spring temporal coverage. In particular, the campaign was partitioned into 3 intensive measurement phases. The first phase was set in late November and early December 1999 as the polar vortex set up, and as temperatures typically fall below about 195K (the nitric acid trihydrate saturation temperature) over wide regions. The second phase was chosen during the period when polar lower stratospheric

temperature are usually lowest and the vortex is at its strongest. Because this phase was timed to the coldest period, expected formation of PSCs would lead to extensive conversion of chlorine into reactive forms. The final phase of SOLVE-THESEO 2000 was timed to the recovery period of the polar vortex as temperatures rose above 195K, the vortex decreased in strength, and perturbed chemistry began to recover.

The science requirements prescribed a need for regular and deep penetrations of the polar vortex along with good proximity to the coldest portion of the polar vortex. Kiruna, Sweden provided an ideal site for SOLVE-THESEO 2000's principal activities. The Arena Arctica hangar at the Kiruna airport was built in 1992 as a facility for accommodating large aircraft field projects on environmental issues. In late January, this hangar simultaneously accommodated the NASA ER-2, NASA DC-8, and DLR Falcon. A second hangar was available for use by the ARAT and Lear Jet. The Arena also includes offices, labs and shared rooms such as a pantry, a meeting room, dressing rooms, and workshops. The lab and office space on either side of the hangar housed all of the investigators and instruments for the aircraft portion of the campaign.

Balloon operations were conducted at the Swedish Space Corporation's Esrange facility, which is approximately 40 km from Kiruna. This facility is able to launch balloons of up to 1,000,000 m^3. The facility includes a large 400 meter by 250 meter launch pad, a balloon control facility, and a laboratory and payload assembly building (the cathedral). In addition, Esrange includes accommodation and dining facilities to handle the large teams of scientists associated with the balloons. A second balloon facility, where 10,000 m^3 balloons were launched, was at the Norwegian Rocket Range at Andøya.

SOLVE-THESEO 2000 operations extensively covered the Arctic region. Figure 1 displays this operational region. The magenta line indicates the 2700 km distance from Kiruna, roughly the operational radius of ER-2 flights. Kiruna is located at the center of the image by the green star. Ozone-sonde launch sites were widely distributed across the polar region (as indicated by the red points on Figure 1). In addition, ground-based instruments were located at a number of sites across the polar and mid-latitude region in support of SOLVE-THESEO 2000. The observational sites in the EU project Compilation of atmospheric Observations in Support of Satellite measurements over Europe (COSE – coordinator: M de Mazière, BISA) are shown as the blue points in Figure 1.

2.2 Platforms

The SOLVE-THESEO 2000 campaign had a mix of observational platforms that included satellites, ground stations, aircraft, and balloons.

2.2.1 Satellites

Satellite observations provided a wide view of the Arctic polar vortex over the course of the 1999/2000 winter. These observations were vital to following the hemispheric evolution of ozone, PSCs, and temperatures over the course of the winter. The satellite observations provided a first look at the basic structure of these fields. These maps assisted in the flight planning, day-to-day launch schedules, and real-time analysis of observations. Five satellite instruments were principally used during the campaign: GOME, POAM, HALOE, TOMS, and SAGE II. In addition, the UARS MLS instrument was turned on for two short periods during the winter.

2.2.1.1 POAM

The POAM III instrument was launched onboard the French SPOT 4 spacecraft on March 24 1998, into a sun-synchronous 98.7°E inclination orbit (PI: R. Bevilacqua, NRL). The POAM III instrument is a nine-channel visible/near infrared photometer (352-1020 nm) for measuring trace constituents in the stratosphere using solar occultation. The POAM III measurements include O_3, H_2O, NO_2, and aerosol extinction. A detailed description of the POAM III instrument, and early validation results are given by Lucke *et al.* [1999]. POAM III makes 14 measurements per day in each hemisphere evenly spaced in longitude around a circle of latitude. The latitudes of the POAM occultations are shown in Figure 2 as the magenta line. Because of the polar vortex's size, this sampling pattern allows POAM to obtain profiles both inside and outside the Arctic polar vortex on a daily basis throughout the winter.

2.2.1.2 TOMS

The Total Ozone Mapping Spectrometer (TOMS) instruments have been in nearly continuous orbit since late 1978. The first TOMS was launched aboard the Nimbus-7 spacecraft, while the latest TOMS on the Earth Probe satellite was launched on July 2, 1996. The TOMS instrument uses 6 wavelengths (360.0, 331.2, 322.3, 317.5, 312.5, and 308.6 nm) in the UV portion of the spectrum to derive total column ozone amounts. The side-to-side instrument scanning, combined with the 39 km by 39 km nadir field-of-view yields complete daily coverage of total ozone across the globe. Because the TOMS instrument requires backscattered solar radiation, observations are not available in polar night. Figure 2 displays the longitudinally averaged (zonal mean) TOMS observations over the

period of October 1999 through April 2000. Measurements are not available for solar zenith angles greater than 82°.

2.2.1.3 GOME

The Global Ozone Monitoring Experiment (GOME) was launched on April 21, 1995 on board the second European Remote Sensing Satellite (ERS-2) [Burrows *et al.*, 1999 and references therein]. GOME is a nadir-scanning spectrometer that measures the solar radiation scattered by the atmosphere and the extra terrestrial solar irradiance in the ultraviolet and visible spectral region. The entire spectral region between 230 and 790 nm is observed at moderate spectral resolution of 0.2 to 0.4 nm in four individual linear detector arrays each having 1024 detector pixels. The field of view may be varied in size from 320 km by 40 km to 40 by 40 km for a 1.5 s measurement. For O_3 profiling a 12 second swath is typically used, corresponding to eight 1.5 s measurements or 960 km x 80 km. The ERS-2 orbit is a sun synchronous orbit having an equator crossing time of 10:30 am. As a result GOME obtains full global coverage over a three-day period at the equator. As with TOMS, GOME relies on backscattered solar radiation, hence, it can only make measurements outside the region of continuous polar darkness. GOME products for the SOLVE-THESEO 2000 campaign include column O_3, BrO, NO_2, OClO, and H_2CO and O_3 profiles.

2.2.1.4 UARS HALOE

The HALogen Occultation Experiment (HALOE) is part of the Upper Atmospheric Research Satellite (UARS) which was launched on September 12, 1991 into a 57° inclined orbit (PI: J. M. Russell III, Hampton Univ.). HALOE measures the absorption of solar energy due to stratospheric trace gases during spacecraft sunrise and sunset events. Vertical scans of the atmosphere are obtained by tracking the sun position during 15 sunrise and 15 sunset occultations per day. The instantaneous vertical field of view is 1.6 km. Daily retrievals are at approximately equal latitudes with a 24° longitudinal resolution. Latitudinal sweeps occur approximately once every 30 days. The HALOE altitude range is 15 km to 60-130 km, depending on the species. Vertical profiles of O_3, H_2O, NO_2, temperature, and pressure are obtained using broadband techniques. Vertical profiles of HCl, HF, CH_4 and NO rely on gas filter radiometer techniques [Russell *et al.*, 1993]. Aerosol extinction coefficient profiles and sulfate aerosol surface area densities (SAD) are inferred [Hervig *et al.*, 1996].

Version 19 (third public release) of the HALOE retrieval was used during SOLVE-THESEO 2000. HALOE made extensive observations of the early vortex formation during October and November 1999 with 18% of the northern hemisphere HALOE observations occurring within the Arctic proto-

vortex. Figure 2 displays the HALOE occultations for both sunrise (blue crosses) and sunset (blue stars). From mid February to mid March HALOE returned to high northern latitudes and once again made some vortex observations.

2.2.1.5 SAGE II

The SAGE II (Stratospheric Aerosol and Gas Experiment II) sensor was launched into a 57° inclination orbit aboard the Earth Radiation Budget Satellite (ERBS) in October 1984. During each sunrise and sunset encountered by the orbiting spacecraft, the instrument uses the solar occultation technique to measure attenuated solar radiation through the Earth's limb in seven channels centered at wavelengths ranging from 0.385 to 1.02 micrometers. The exo-atmospheric solar irradiance is also measured in each channel during each event for use as a reference in determining limb transmittances.

The transmittance measurements are inverted using the "onion-peeling" approach to yield 1 km vertical resolution profiles of aerosol extinction (at 0.385, 0.453, 0.525, and 1.02 μm), O_3, NO_2, and H_2O. The focus of the measurements is on the lower and middle stratosphere, although retrieved aerosol, H_2O, and O_3 profiles often extend well into the troposphere under non-volcanic and cloud-free conditions.

The sampling coverage for SAGE II varies in latitude from approximately 60°N to 80°S during the winter. The SAGE II measurements provide insight into the distribution of aerosol, O_3, and H_2O found at mid and low latitudes outside to polar vortex. A detailed description of SAGE II can be found in McCormick *et al.* [1979] and Cunnold *et al.* [1991].

2.2.1.6 UARS MLS

The Microwave Limb Sounder (MLS) on UARS (PI: J. Waters, JPL) observes microwave emission from Earth's limb to measure vertical profiles of selected chemical species and temperature. Waters [1993] describes the measurement technique, and Waters *et al.* [1999] summarize results obtained through 1999. The instrument [Barath *et al.*, 1993] operates at 63, 183, and 205 GHz; its calibration is described by Jarnot *et al.* [1996].

MLS was in standby mode for most of 1999-2000. It was operated 2-13 February and 27-29 March 2000 to measure Arctic ClO, HNO_3, and O_3 with the 205 GHz radiometer [Santee *et al.*, 2000].

2.2.2 Ground stations

A total of 20 ground stations with 51 instruments were involved in the SOLVE-THESEO 2000 campaign. Lidars, SAOZs, Dobsons, DOASs, microwave radiometers, FTIRs, ozone-sondes, and backscatter-sondes provided continuous profiles of O_3, ClO, N_2O, CH_4, HNO_3, NO, HCl, HF, aerosol, and wind as well as columnar densities of O_3, ClO, N_2O, CH_4, HNO_3, NO, HCl, HF, NO_2, BrO, CO, $ClONO_2$, COF_2, and OClO. Most lidars also measured temperature at high altitude (<10 hPa). Table 1 lists the sites and observations.

2.2.3 Aircraft

Six aircraft were employed during the SOLVE-THESEO 2000 campaign. The SOLVE campaign provided the NASA ER-2 and the NASA DC-8, while the THESEO 2000 campaign provided the French ARAT, the DLR Falcon, the Swiss Learjet, and the French Mystère 20 aircraft.

2.2.3.1 ER-2

The NASA ER-2 is the civilian version of the U-2 spy plane. NASA has employed the ER-2 on numerous field campaigns. The aircraft is capable of flights at altitudes over 20 km (pressures less than 50 hPa) for durations up to 8 hours. The ER-2 was flown 13 times during the 2nd and 3rd phases of the campaign, including transits into and from Kiruna. The aircraft is shown in Figure 3, with the locations of the 17 instruments. The ER-2 instruments are listed in Table 2 along with the PI, home institutions, and measurement focus.

2.2.3.2 DC-8

The NASA DC-8 was a commercial airliner that has been converted into a flying laboratory. Like the ER-2, the DC-8 has been deployed on numerous field campaigns for investigating stratospheric ozone. The aircraft is capable of flights to about 12 km for durations over 10-hours. The DC-8 was flown 23 times during the 3 campaign phases. The aircraft is shown in Figure 4, with the locations of the 17 instruments. The DC-8 instruments are listed in Table 3 along with the PI, home institutions, and measurement focus.

2.2.3.3 ARAT

The ARAT is a turbo-prop Fokker 27-MK 700 aircraft that carries the LEANDRE backscatter lidar (PI: C. David of CNRS-SA/IPSL). The ARAT is capable of flight to approximately 5 km, and

durations of 4 hours. The ARAT aircraft is a research facility jointly operated by the Institut National des Sciences de l'Univers (INSU-CNRS), the French Space Agency (CNES), the French National Weather Center (Météo-France) and the National Geographic Institute (IGN). LEANDRE is a backscatter lidar emitting 10 pulses per second at a wavelength of 532 nm. The backscattered signal is split into components polarized parallel and perpendicular to the laser emission. The ARAT flew on January 25 2000 in coordination with the second PSC-Analysis balloon. Two flights were performed. The first flight was upstream towards Andøya, before the PSC-Analysis gondola launch, while the second flight was directed southeastward between Kiruna and Rovaniemi. During this second flight, the position of the balloon was communicated in real time to the ARAT through the VHF station in Esrange, allowing the aircraft to track the balloon efficiently. PSCs were observed between about 20 and 25 km in altitude. The ARAT also flew on January 26 and 27 2000.

2.2.3.4 Falcon

The DLR Falcon 20-E5 is a modified twin engine-jet business aircraft capable of flights to 13.7 km with a maximum endurance of up to 5 hours. The Falcon carried the OLEX lidar during the SOLVE-THESEO 2000 campaign. OLEX (PI: H. Flentje, DLR) measures ozone as well as depolarization- and wavelength-resolved backscatter of aerosol and PSCs. During the 2nd phase of SOLVE-THESEO 2000 there were 8 science flights (including 2 transit flights) of the FALCON lidar. Three of them were mountain wave flights, the other three probed the large nitric acid trihydrate (NAT) PSCs south of Spitzbergen. On January 27 the FALCON precisely tracked two balloons (HALOZ and TRIPLE), which carried various *in situ* aerosol probes. Figure 5 displays the DLR Falcon parked on the ramp outside of the Arena Arctica on January 31 2000.

2.2.3.5 Lear Jet

The Swiss Air Force Learjet carried a microwave radiometer (PI: N. Kämpfer, University of Bern). The measurements were made from March 8 to 14, 2000. This instrument recorded spectra of stratospheric water vapor at 183 GHz as well as ozone at 176 GHz. From these spectra, profiles were derived over an altitude range of roughly 20-70 km. Several flights were performed, including Kiruna to Iceland, Kiruna to the North Pole, and Kiruna to the North Atlantic. After the Arctic flights, the plane flew south to the Canary Islands to extend the latitude range of the measurements to the subtropics.

2.2.3.6 Mystère 20

The French Mystère 20 is a twin turbofan engine aircraft built by Dassault. The Mystère is capable of 3-hour flights to a maximum altitude of approximately 13 km, and a range of approximately 1800 km. During SOLVE-THESEO 2000, the Mystère carried the Alto ozone lidar (PIs: S. Godin and A.Hauchecorne, CNRS-SA / IPSL) which is a DIAL system capable of measuring ozone profiles from 1 km above the plane to about 20 km. The objective for the Mystère was to measure polar ozone filaments that were breaking off of the polar vortex. The Mystère was flown on February 28, March 7, March 26, and March 28 2000 and was operated from Creil airport near Paris.

2.2.4 Balloons

2.2.4.1 OMS *in situ*

The NASA OMS *in situ* payload was launched on November 19 1999 and March 5 2000, with both flights inside the Arctic vortex. *In situ* measurements of the vertical profiles of a range of atmospheric tracers were made. The OMS *in situ* gondola includes the following instruments:

- The Airborne Laser Infrared Absorption Spectrometer (ALIAS-II). HCl, CH_4, N_2O (PI: C. Webster, JPL)
- The Dual-beam UV in situ O_3 Photometer (PI: J. Margitan, JPL)
- The High-Altitude Fast-Response CO_2 Analyzer (PI: S. Wofsy, Harvard)
- The Lightweight Airborne Chromatograph Experiment (LACE) described by Moore *et al.* [2001]. CFC-11, CFC-12, CFC-113, halon-1211, $CHCl_3$, CH_3CCl_3, CCl_4, SF_6 and N_2O (PI: J. Elkins, NOAA/CMDL)

The Frost-Point Hygrometer was launched as a free flying package in parallel with the OMS *in situ* payload (PI: S. Oltmans, NOAA/CMDL)

2.2.4.2 OMS Remote

The OMS Remote payload consisted of two instruments. The JPL MkIV infra-red interferometer (PI: G.Toon, JPL) made profile measurements of a wide range of species in solar absorption mode by observing sunrise or sunset from a balloon. These included H_2O, O_3, N_2O, CO, CH_4, NO, NO_2, HNO_3, HNO_4, N_2O_5, H_2O_2, $ClNO_3$, HOCl, HCl, HF, COF_2, CF_4, SF_6, CFC-11, CFC-12, CCl_4, CH_3Cl, and CO_2. The Submillimeterwave Limb Sounder (SLS) is a heterodyne radiometer measuring thermal emission spectra (PI: R.Stachnik, JPL). It measured atmospheric profiles of ClO, O_3, HCl, HNO_3 and N_2O. This payload made two flights, both inside the Arctic vortex. The first was early in

the winter on December 3 1999, and the second was on March 15 2000 just prior to a major split in the vortex.

2.2.4.3 MIR

The Montgolfière Infrarouge (MIR) packages (PI: J-P. Pommereau, CNRS-SA) are long duration balloons. The objective of the flights was to complement the measurements of 1999 by two new instrumented scientific MIR flights in the vortex as well as an additional technical MIR, all carrying payloads recovered in 1999. The first two MIRs were launched on the same day (February 18 2000) when the vortex passed rapidly above Kiruna. They lasted for 2 and 18 days, both being automatically cut-down when reaching 55°N. Their payloads were recovered respectively in the Hudson Bay and in Belarus near Minsk. The third (technical) balloon failed during the initial ascent and no useful measurements were made. The data include temperature, pressure, altitude and IR radiation measurements every 15 minutes along the two flights, five CH_4 and H_2O profiles, and ten O_3, NO_2 and OClO profiles.

2.2.4.4 PSC analysis

The PSC analysis balloon borne payload was launched from Esrange on January 19 and January 25 2000 for detailed studies of polar stratospheric cloud (PSC) particles (see Figure 6). The payload consisted of a mass spectrometer with an aerodynamic focusing lens for condensed phase chemical analysis (ACMS, PI: J. Schreiner, MPIK), aerosol counters for condensation nuclei and aerosol > 0.3μm for PSC particle size distributions (PI: T. Deshler, Univ. of Wyoming), backscatter-sondes for observations of optical properties and physical phase (PIs: A. Adriani, CNR-IFA; J. Rosen, Univ. of Wyoming; and N. Larsen, DMI), and a water vapor frost point hygrometer (PI: J. Ovarlez, LMD). The balloon altitude was controlled by CNES and on each flight the balloon went up and down, passing through PSC layers multiple times.

2.2.4.5 HALOZ

A series of five small balloons carrying instruments to address the issue of halogen-catalyzed ozone loss (HALOZ) were launched from Kiruna, Sweden in between January and April 2000. A critical subset of species involved in ozone loss were measured *in situ* with lightweight instruments. ClO and BrO were measured using a resonance fluorescence instrument (PI: D. Toohey, Colorado Univ.); particle number and size distributions were measured by optical scattering (PI: T. Deshler, Univ of Wyoming); and CFC-11 was measured by the *in situ* gas chromatograph, DIRAC (PI: A. Robinson,

Univ. of Cambridge). Ozone was measured by an ozone-sonde. Two distinct payload configurations were used for maximum launch flexibility. The first, which consisted of all the instruments, was launched twice (January 19 and January 27, 2000) when PSCs were observed visually. For the last three flights (March 1, March 8 and April 4), the particle instruments were removed. On March 1 and April 4, CFC-11 was measured by the DESCARTES grab-sampler (PIs: H. Nilsson, IRF, and F.Danis, Univ. of Cambridge) rather than DIRAC. All flights took place inside the vortex.

2.2.4.6 Triple

The TRIPLE payload included a ClO/BrO chemical conversion resonance fluorescence instrument (PI: F. Stroh, FZ Jülich), the cryogenic whole air sampler BONBON which measures a wide range of stable gases including N_2O, CFCs, CH_4, HCFCs and SF_6 (PIs: A. Engel and U. Schmidt, Univ of Frankfurt), the Lyman-alpha hygrometer FISH [Zöger *et al.*, 1999], the filter UV radiometers [Schiller *et al.*, 1994] (PI of both: C. Schiller, FZ Jülich), and an instrument measuring aerosol size distribution [Ovarlez and Ovarlez, 1995] (PI: J. Ovarlez, CNRS-LMD). This payload was flown on 27 January, 2000 and 1 March, 2000 from ESRANGE, separated by a few hours from the HALOZ flights.

2.2.4.7 LPMA/DOAS

The LPMA/DOAS payload was launched from Esrange on February 18 2000. Solar absorption measurements were performed by the FTIR (Fourier Transform-InfraRed Spectrometer – PI: C. Camy-Peyret, UPMC) and DOAS (Differential Optical Absorption Spectrometer – PI: K. Pfeilsticker, Univ. Heidelberg) instruments. These spectrometers simultaneous measured vertical profiles of HCl, $ClONO_2$, CH_4, N_2O, HNO_3, NO_2, NO, O_3 and HF in the infrared spectral range and O_3, BrO, IO, NO_2, O_4, OClO and OIO in the UV-visible spectral range.

2.2.4.8 SALOMON

SALOMON is a UV-Visible spectrometer (350 - 700 nm) which uses the moon as the light source. The instrument (PI: M. Pirre, LPCE) measures the vertical distributions of O_3, NO_2, NO_3, OClO, aerosol extinction coefficients, and possibly OBrO. Two SALOMON flights were performed in different geophysical conditions, allowing a comparison of various aspects of the stratospheric polar chemistry to be made. The first flight was on January 23 2000 at the edge of the vortex. The flight was stopped early for safety reasons and observations were made in the 13-20 km range. The second

flight occurred on February 22 2000. The measurements were made in warm conditions outside the polar vortex. The full moon-rise was observed, giving profiles between 16 and 30 km.

2.2.4.9 Micro-Radibal

Micro-Radibal is a balloon-borne instrument developed to study stratospheric aerosols and measures the radiance and polarisation of scattered sunlight at 730, 865, 1000, 1620 nm (PI: C. Brogniez, U. Lille). The gondola rotates around a vertical axis and observations are made under various scattering angles during the ascent of the balloon. Micro-Radibal flew on 26 January, 2000 from Esrange and made measurements between 13 and 23 km.

2.2.4.10 SAOZ balloon flights

The SAOZ (PIs: J-P. Pommereau, F. Goutail, CNRS-SA) is a UV-visible spectrometer that measures in the wavelength region between 300-600 nm. During SOLVE-THESEO 2000 6 flights were made inside the vortex and 2 flights outside. The basic SAOZ provides O_3, NO_2 and OClO vertical profiles. A UV-enhanced version, SAOZ-BrO, provided BrO and OClO vertical profiles on 3 flights inside the vortex, and on all flights outside vortex. One flight inside the vortex was made in parallel with a HALOZ flight to allow a comparison with the ClO/BrO resonance-fluorescence instrument. In addition, tracer profiles were measured on all flights with either the DESCARTES (PIs: H. Nilsson, IR; and F.Danis, Univ. of Cambridge) or DIRAC (PI: A. Robinson, Univ. of Cambridge) instruments or the methane TDL instrument (PIs: R. Jones, Univ. Cambridge; and P. Woods, NPL). In total, DESCARTES made 11 flights during this winter, ten in conjunction with other instruments (OMS remote; HALOZ; OMS *in situ*; SAOZ) and one solo flight in early winter (November 11 1999). DIRAC made four flights in conjunction with other instruments (three with HALOZ and one with OMS *in situ*). These flights were made to facillitate comparisons with the OMS *in situ* measurements.

2.2.5. Ozone-sonde stations

During SOLVE-THESEO 2000, over 650 ozone-sondes were launched from a network of 36 stations in 20 countries at mid and high latitudes in the northern hemisphere (see Figure 1). Many of these stations were underneath the Arctic vortex at various times, and so a high proportion of the ozone-sondes made measurements inside the Arctic vortex. The ozone-sondes were either part of regular programs or were launched in response to requests within the coordinated Match program or in conjunction with aircraft or balloon flights.

2.3 Flights and launches

The SOLVE-THESEO 2000 campaign was divided into 3 intensive measurement phases. The flight log is shown in Table 4.

The principal deployment site was in Kiruna, Sweden (see Figure 1 to view operational region of SOLVE-THESEO 2000). Five aircraft were primarily staged from the Arena Arctica at the Kiruna airport, while all of the Mystère 20 flights were from a small airfield near Paris. The balloons were primarily flown from Esrange, though two additional SAOZ balloons were flown from Andøya, Norway (240 km northwest of Kiruna)

The aircraft flights indicated in Figure 7 cluster into the 3 phases of the campaign. The balloon flights are shown in Figure 8, superimposed on the polar vortex temperatures. As planned, the first phase sampled the polar vortex during the vortex formation phase as temperatures cooled below the NAT saturation temperature of 195 K. The 2nd phase occurred shortly after the coldest period during the 1999-2000 winter in the last two weeks of January. The final phase occurred as temperatures warmed to temperatures greater than 195K.

2.4 Mission forecasting

The aircraft platforms and balloon payloads discussed in the previous sections provided an enormous capability for understanding the Arctic polar vortex. However, such resources required careful coordination and direction for optimizing the scientific return. Optimized flights were determined using meteorological, chemical, and microphysical forecasting. A number of meteorological and theory groups participated in the SOLVE-THESEO 2000 campaign. Over the course of the campaign these groups held daily meetings at Arena Arctica and Esrange to discuss the evolving polar vortex and forecast its further evolution. In addition, tropospheric forecasts were used to determine flight conditions, particularly for the large balloon payloads and NASA ER-2.

2.4.1 Tropospheric forecasting

The surface weather forecasting for SOLVE-THESEO 2000 at the Arena Arctica was conducted by Dr. G. Forbes (The Weather Channel). Forecasting for the DC-8, ARAT, Falcon, and Lear Jet was relatively straightforward, since these aircraft have a near "all-weather" flight capability. However, the NASA ER-2 has rather severe weather restrictions. For example, the ER-2 requires runway cross winds to be less than 12 knots (6 m/s), wind chill temperatures greater than –31°C, good visibility,

low ceilings, and a runway that is relatively free of ice and snow. Such conditions were satisfied relatively often in Kiruna, but were extremely difficult to forecast.

Surface forecasting at Esrange was handled by the U. S. National Science Balloon Facility (NSBF) staff meteorologists (G. Rosenberger, J. Hobbie, and R. Mullenax) for the SOLVE OMS launches, and by CNES meteorologists (P. Dedieu and colleagues) for the THESEO 2000 launches. Because of the large size of these balloons, very light surface winds and very small vertical wind shears over the lowest few hundred meters are necessary for safe launches. Forecasting support was also provided by Esrange staff, and sounding balloon launches were handled by the Esrange balloon launch crew. Trajectory forecasts were an important aspect of the balloon launches. These trajectories ensured that the payloads were inside the vortex, and had the desired float times. For example, the second OMS remote launch required very accurate predictions of time to float (a heavy cirrus cover caused an unfavorable radiation environment). The NSBF meteorologists' use of the SINBAD model was critical in determining the launch window. Similarly, the accurate ground wind forecasts from the Meteo-France Arpège model and from SMHI were essential in the launch of the first PSC Analysis gondola. All of the trajectory and meteorological forecasts were prepared with considerable assistance by the Esrange Range Safety team (T. Hedqvist, S. Kemi, and B. Sjoholm).

2.4.2 Stratospheric forecasting

The forecasting for the stratosphere was carried out by a number of groups. These groups used standard meteorological analyses combined with specialized products to predict stratospheric temperatures, the position of the polar vortex, mountain wave amplitudes and turbulence, PSC microphysics, and the chemical composition of the stratosphere.

2.4.2.1 Stratospheric meteorology & mountain wave forecasting

A number of conventional meteorological forecasts and analyses were utilized for SOLVE-THESEO 2000 forecasting. These forecasts and analyses were routinely provided for flight planning and data analysis. Typically, the data were used to forecast the locations of cold temperature regions (for PSC flights), and for locating the position of the polar vortex. These analyses included GSFC Data Assimilation Office GEOS-3 output (PI: S. Strahan), the NCEP/CPC analyses and NCEP/MRF forecasts and analyses (PI: L. Lait, GSFC), the NCEP/AVN output (PI: A. Tuck, NOAA-AL), the Australian Bureau of Meteorology's Global ASsimilation and Prediction (GASP) system's analyses and forecasts (PI: D. Waugh), and the ECMWF forecasts and analyses (PIs: G. Braathen, NILU; A. Dörnbrack, DLR; and B. Knudsen, DMI). The Meteo-France ARPEGE model was used for

stratospheric as well as tropospheric forecasting. The UKMO UARS analyses were also used to support the analysis of SOLVE-THESEO 2000 observations. Free University of Berlin subjective analyses of radiosondes were provided for analysis purposes (PI: B. Naujokat, FUB).

A number of specialized products were utilized for forecasting and analysis. High density trajectory model runs based on analyzed and forecast winds were used to predict air masses that had broken off of the polar vortex, had encountered PSCs, had persistently been in polar darkness, or had encountered upper tropospheric clouds. Such trajectory runs based on forecast and analysis products were produced using the NCEP and DAO forecasts (PI: L. Lait), the DAO data in combination with NCEP/MRF analyses in the upper troposphere and lower stratosphere for studying water vapor transport (PI: H. Selkirk), the GASP data (PI: D. Waugh), and the MIMOSA model at CNRS (PI: A. Hauchecorne). Vortex filaments were also forecast using the Chemical Lagrangian Model of the Stratosphere (CLaMS – PI: R. Müller, FZ Jülich).

The Match project [Rex *et al.*, 2001] provided real-time trajectory analyses during the campaign. The main goal was to track and to forecast the motions of air masses that have been probed by ozone-sondes and to enable subsequent ozone measurements within these air masses in a Lagrangian sense. Close coincident measurements of ozone-sondes with the ER-2 instruments were also coordinated based on the ER-2 flight plans and short trajectory forecasts of the motions of the air masses probed along the envisaged flight track. After each ER-2 flight the motions of air masses probed along the actual flight track were tracked and forecast by continuously updated trajectory calculations over ten days. The positions of the air masses probed during previous flights were made available for flight planning and for the coordination of Lagrangian ozone-sonde measurements.

Mountain forced gravity waves are extremely important for understanding the evolution and formation of PSCs, but also for forecasting turbulence that posed a hazard to the NASA ER-2. Forecasts of mountain wave vertical displacement amplitudes, temperature amplitudes and turbulence were provided using the Naval Research Laboratory Mountain Wave Forecast Model (MWFM) interfaced to forecast winds and temperatures from the DAO GEOS-2 forecasts and the U. S. Navy's NOGAP model forecasts (PI: S. Eckerman, NRL). Flow fields and temperature perturbation for the whole of Scandinavia were provided based upon the regional MM5 model (PI: A. Dörnbrack, DLR) and the analagous HRM model (PI: H. Wernli, ETH-Zürich). In addition the HRM model was used to provide forecast trajectories for the TRIPLE payload (see 2.2.4.6). The 3D University of Wisconsin Non-hydrostatic Modeling System (UW-NMS) was used to investigate transport processes at the mesoscale to synoptic scale in the upper troposphere/lower stratosphere near Scandinavia. The 3DVOM is a finite-difference numerical code designed for high-resolution simulations (PI: S. Vosper,

Univ. Leeds). Finally, the flow fields and temperature perturbation over northern Scandanavia were also calculated using the 15 km resolution German Weather Service NWP model.

2.4.2.2 Chemical & Radiative modeling

While the meteorology provided the broad strategy for the campaign, chemical and radiative models provided supplemental information for designing flight paths. Three 3-dimensional (3-D) chemical transport models (CTMs) were employed during SOLVE-THESEO 2000. The GSFC CTM uses DAO GEOS-2 meteorology to provide a full suite of trace gas measurements, including source gases, reservoir species, and radical species in all of the major families (PI: R. Kawa). The UK UGAMP SLIMCAT model is an isentropic 3-D CTM that uses UKMO meteorology to provide a full suite of trace gases (PIs: M. Chipperfield, Univ. Leeds; and J. Pyle, Univ Cambridge). The REPROBUS model is a full 3-D CTM that uses the Meteo-France ARPEGE analysis and forecast winds to produce a complete set of stratospheric species (PI: F. Lefèvre, CNRS-SA).

In addition to the 3-D models, a chemical trajectory model was run for each of the ER-2 flights (PI: R. Kawa), and for parcels within the polar vortex (PI: K. Drdla) using the GSFC trajectory model. A photochemical steady state model was heavily utilized for forecasting the behavior of radical species under a variety of conditions (PI: R. Salawitch, JPL). A radiative transfer model was extensively used to provide photolysis rate coefficients or j–values for photochemical reactions of interest in the lower stratosphere and upper troposphere, calculated along the ER–2 and DC–8 flight tracks for each flight (PI: S. Lloyd).

2.4.2.3 Microphysical modeling

Determining the evolution and properties of PSCs was a principal goal of the SOLVE-THESEO 2000 campaign. While temperature forecasts were the principal tools for locating prospective regions of PSC formation, microphysical models were employed for real-time analysis of the observations in order to re-direct our strategies while we were in the field. The Integrated Microphysics and Aerosol Chemistry on Trajectories (IMPACT) model was used to simulate PSCs and their impact on stratospheric chemistry (PI: K. Drdla). The MM5 results from the DLR and the HRM trajectories were used with the Mainz microphysical box model [Meilinger *et al.*, 1995; Tsias *et al.*, 1997; Carslaw *et al.*, 1998] for calculation of PSC temporal evolution along air parcel trajectories.

3.0 Results

As described in section 2.1, the SOLVE-THESEO 2000 campaign was partitioned into 3 phases: 1) the early December polar vortex set-up period; 2) the very cold, late January period; and 3) the vortex recovery period. As will be shown, all 3 phases were adequately covered as had been hoped. Ground-based, satellite and ozone-sonde measurements provided continuous coverage throughout the winter, and filled the observational gaps between the phases.

The first phase of SOLVE-THESEO 2000 was timed to occur in early winter as temperatures cooled to the point where PSCs would form. Balloon flights and the NASA DC-8 flights were prioritized to understand the initial conditions of the polar vortex prior to the occurrence of significant PSCs, and to measure some of the first appearances of PSCs. Initial flights of the DC-8 and the OMS remote payload did not reveal elevated levels of ClO, suggesting that the first goal was achieved [Bremer *et al.*, 2001]. In addition, a number of early PSCs were detected by the DC-8 in flights over the high Arctic during the course of the first two week phase.

The second phase was planned to occur in mid-winter when temperatures were at their lowest. In reality, the aircraft and balloon flights were all conducted shortly after the coldest period in the 1999-2000 winter. All of the flights inside the polar vortex encountered air that had been chemically perturbed by PSCs. In addition, vast regions of the polar vortex were still cold enough in this late January period to contain PSCs.

The final campaign phase was set for the first two weeks of March to investigate the recovery of the polar vortex. Surprisingly, at the start of this phase the polar vortex was quite strong and temperatures were still cold enough to form PSCs. Again, both chemically perturbed air and PSCs were measured inside the polar vortex during this phase.

3.1 Meteorological Background

The early stratospheric winter of 1999-2000 has been described in Manney and Sabutis [2000]. In this paper they point out the unusually cold early winter lower stratosphere, and describe the vortex evolution in 1999-2000 as typical. The breakup of the 1999-2000 lower stratospheric vortex occurred on April 11, 2000, slightly later than the average breakup date of March 29 [Waugh and Rong, 2001].

3.1.1 Temperatures

The temperature of the polar vortex over the course of the 1999-2000 winter has been shown in Figure 1 of Manney and Sabutis [2000]. The vortex averaged temperature is shown in Figure 8 of this

paper with all of the SOLVE-THESEO 2000 balloon flights. The first balloon flights and the DC-8 flights occurred as the vortex was cooling below 195 K during the first phase of the campaign. Lidar temperature observations inside the vortex, ozone-sondes, and conventional radiosondes all provided direct evidence of this cold polar vortex in the mid-to-lower stratosphere of the Arctic during this early winter phase.

Figure 8 shows that the coldest temperatures occurred in the first two weeks of January, immediately prior to the second phase of the campaign. Again, direct observations provide an independent validation of these cold lower stratospheric temperatures. Extensive measurements of PSCs were obtained during this second phase.

During the final phase of SOLVE-THESEO 2000, the polar lower stratospheric temperatures increase above 195 K. Again, Figure 8 displays this increase during the first two weeks of March. During the final flights of the DC-8 from Kiruna, temperatures were observed to be too warm for the formation of PSCs.

3.1.2 Vortex and jet evolution

The lower stratospheric polar vortex developed slowly during the 1999-2000 winter [Manney and Sabutis, 2000], reached its greatest strength in mid-January, and broke apart in mid-April [Waugh and Rong, 2001]. This evolution is illustrated in Figure 9 which displays the average wind on the 600 K isentropic surface following lines of equivalent latitude (equivalent to a zonal mean in a vortex centered coordinate system). In the mid-stratosphere, the polar night jet-core speed was greater than 20 m/s by early-November, 30 m/s by early-December, and 50 m/s by late-December. The polar vortex is the region contained by this polar night jet. This jet had three periods of deceleration: late-January to early-February as the jet narrowed in latitudinal dimension (indicated by D on Figure 9), mid-March as the jet decelerated and the polar vortex shrank (F on Figure 9), and early-April as a greatly reduced vortex disappeared completely (H on Figure 9). The first SOLVE-THESEO 2000 phase took place as the vortex was rapidly accelerating (B on Figure 9). The second phase occurred as the vortex decelerated and narrowed (D on Figure 9), while the third phase occurred as the vortex was rapidly shrinking (F on Figure 9). The thick black line on Figure 9 shows the equivalent latitude of Kiruna on this 600 K isentropic surface. Generally, Kiruna's equivalent latitude is poleward of the jet core, hence Kiruna was usually inside the polar vortex over the course of the 1999-2000 winter. Kiruna is outside the vortex during mid-February and late-March (aside from the spin-up and break-down periods of the vortex). At lower stratospheric altitudes (e.g., 450 K), the vortex is more variable, and Kiruna was found to be frequently outside of the vortex.

The behavior of the polar night jet in Figure 9 can be broadly explained by examining the wave energy propagating out of the troposphere and into the stratosphere over the course of the campaign. The large wave events act to decelerate the jet, and warm the polar vortex [Newman *et al.*, 2001]. The wave energy that drives the circulation of the stratosphere is proportional to the eddy heat flux for large-scale waves (superimposed on Figure 9 as the white line, scale on the right hand side of the figure). There are 4 important bursts of wave energy (large eddy heat flux) that affect the stratosphere during the 1999-2000 winter. The first burst (indicated by A on Figure 9) acts to both retard the jet development and the radiative cooling of the polar region. The jet builds and the polar region cools as this first event falls off. The second burst (bracketed by C and E on Figure 9) acts to narrow the broad flow and warm the polar vortex from the cold early January temperatures. The third burst (indicated by F) warms the vortex above temperatures necessary for the formation of polar stratospheric clouds and considerably reduces the jet speed and vortex size. The fourth burst in early-April (H on Figure 9) completely breaks-up the vortex.

The potential vorticity evolution in the lower stratosphere generally follows the evolution of the polar night jet. Figure 10 displays a series of potential vorticity maps on the 450 isentropic surface over the course of the winter (modified potential vorticity is used herein, see Lait [1994]). The letters in the titles of each map correspond to the letters shown in Figure 9. Both the November 23 (A) and December 2 (B) panels display the weak vortex that characterized the early lower stratospheric winter. The mid-December to early-March (C, D, E, F) vortex is quite strong and large, while the polar vortex in late March and early April was quite small (G and H). There are three periods of weak eddy heat flux shown on Figure 9 (C, E, and G). These three periods correspond to relatively symmetric polar vortices that are shown in Figure 10.

3.1.3 Total ozone

Total ozone in the Arctic was quite low during spring of 2000. Figure 2 displays the zonal mean total ozone obtained by the Earth Probe satellite's TOMS instrument. During the February-April period, a low of ozone is distinctly observed in the Arctic that is co-incident with the polar vortex. Figure 11 displays the total ozone average for March over the Arctic region (updated from Newman *et al.* [1997]). Total ozone for March 2000 was much lower than normal.

A very low ozone episode, or mini-hole, occurred in late November and early December 1999 over Northern Europe. This was the lowest column ozone values ever measured by TOMS and ground-based instruments in the northern hemisphere during this early part of the cold season. This largely

dynamical ozone reduction was observed to occur in conjunction with (early-winter) polar stratospheric clouds [Hood *et al.*, 2001; Orsolini and Limpasuvan, 2001]. While mini-holes may lead to ozone loss via the formation of cold temperatures and PSCs, they are not caused by ozone loss, and tend to occur during the winter period and are associated with upper tropospheric anti-cyclones systems in the storm track region of the North Atlantic [James, 1998].

3.2 Campaign results

3.2.1 Transport and dynamics

The evolution of the vortex and polar temperatures has been broadly described herein and more precisely in Manney and Sabutis [2000] and the NOAA Climate Prediction Center's Northern Hemisphere winter summary for 1999/2000 [see http://www.cpc.ncep.noaa.gov/products/stratosphere/winter_bulletins/nh_99-00/index.html). Newman *et al.* [2001] quantitatively and theoretically show that the cold stratosphere during the SOLVE-THESEO 2000 campaign was a result of weak tropospheric wave driving of the stratosphere. Waugh and Rong [2001] show the breakup date of the vortex as April 11, 2000.

The vortex breakup and the mixing of air into the mid-latitudes are modeled by Piani *et al.* [2000]. They show that above 420 K most of the air contained in the polar vortex is mixed and carried into low latitudes by the end of June, while air below 420 K was primarily contained in the polar region.

Godin *et al.* [2001] describe the appearance of polar air over the OHP site in Southern France. While the appearance of vortex air over OHP was relatively low compared to the previous 3 years, they estimate a 4% reduction of ozone in the 400-500 K layer as a result of low ozone filaments over OHP. Hauchecorne *et al.* [2001] used a high resolution isentropic model to estimate the transport of ozone to the mid-latitudes in filamentation events coming off of the polar vortex. They found that winters with strong and cold polar vortices are associated with relatively weak filamentation compared to active years when as much as 20% of the vortex is transported to mid-latitudes.

The polar vortex is chemically distinct from the mid-latitudes. Very large gradients of trace gas concentrations are observed in crossing the boundary of the polar vortex, forming chemical "fronts". One of the principal gases used for diagnosing the behavior of the polar vortex is nitrous oxide (N_2O). Hurst *et al.* [2001] describe the development of a high-resolution, consistent, unified N_2O data set derived from the ER-2 *in situ* observations. Such a data set is critical for diagnosing the evolution of

the vortex and understanding tracer-tracer relationships. Greenblatt *et al.* [2001] use the N_2O observations to describe a technique for precisely defining the edge of the polar vortex.

While conventional meteorological observations and models describe the larger scale meteorology, mesoscale models are necessary to also describe the basic thermal structure of the stratosphere. In particular, such models are necessary to describe the smaller scale features that can lead to the formation of PSCs. Dörnbrack *et al.* [2001] describe the model and observations of mountain wave forced PSCs that formed in late January in the Kiruna region.

3.2.2 Formation and composition of PSCs

Because the winter of 1999/2000 was cold, extensive PSCs were observed over the course of the SOLVE-THESEO 2000 campaign. Using POAM III measurements, Bevilacqua *et al.* [2001] give a description of the extent of the PSCs during the entire campaign and they contrast the 1999/2000 observations with previous years. In particular, PSCs were first observed by POAM in mid-November and were last observed on March 15, 2000.

In situ observations of PSCs were made by both aircraft and balloons during the campaign. Fahey *et al.* [2001] describes the measurements of large nitric acid hydrate particles that were found over extensive portions of the polar vortex. These large nitric acid containing particles were found at temperatures above the frost point, and were large enough to considerably de-nitrify the stratosphere. Voigt *et al.* [2001] and Schreiner *et al.* [2001] report the first direct observations of the composition of PSCs by the Kiruna launched PSC gondola on January 25, 2001. This balloon observation showed that liquid ternary particles were seen near frost point, solid NAT near and slightly above NAT equilibrium, and a few large size NAT that were in thin cloud layers below the other cloud layers. The liquid and NAT particle formation has been simulated by Larsen *et al.* [2001], using a detailed microphysical model to represent the simultaneously measured chemical compositions and particle sizes.

Luo *et al.* [2001] discuss the fives types of PSCs observed by the NASA DC-8 Arotel instrument over the course of the SOLVE-THESEO 2000 campaign and derive some of the properties of these PSCs. Von König *et al.* [2001] use a combination of measurements from several remote-sensing instruments mounted onboard the DC-8 to investigate the composition of one polar stratospheric cloud observed on December 7 1999. A good agreement with a NAT composition is found for this PSC.

As a result of the sedimentation of these large nitric acid containing particles, extensive denitrification was observed in the polar vortex. Popp *et al.* [2001] report that the polar vortex has an average denitrification of 60%. Denitrification was also determined by remote observations of odd nitrogen constituents [Kleinböhl *et al.*, 2001]. Corresponding to this denitrification at 17-21 km, Koike *et al.* [2001] report that slight increases in NOy were observed from the DC-8 at 10-12.5 km in March, which are interpreted as being caused by the evaporation of particles after falling from higher altitudes. While extensive denitrification was observed in the vortex, only a small dehydration was observed. *In situ* balloon measurements of H_2O from January until March showed dehydration up to 0.5 ppmv at 20-22 km altitude [Schiller *et al.*, 2001], while ER-2 data at highest flight levels consistently yield a dehydration of 0.2-0.3 ppmv for the vortex as a whole [Herman *et al.*, 2001]. The observations thus provide the first detection of a widespread dehydration in an Arctic vortex.

New techniques for analyzing remotely sensed observations of PSCs have been developed and used in the SOLVE-THESEO 2000 campaign. The t-matrix technique utilized by Luo *et al.* [2001] derives microphysical properties of PSCs using the lidar observations, but assumes that the particles are spheroidal in shape. The finite difference time domain (FDTD) technique of Reichardt *et al.* [2001] derives microphysical properties of PSCs from lidar data assuming that the PSCs are irregular and hexagonal in shape. Strawa *et al.* [2001] derive a new technique for discriminating PSC type 1a and 1b using POAM III satellite observations.

The ability to model accurately the denitrification of the polar vortex by the large NAT particles is critical for future assessments of the stratosphere. A one-dimensional model of this denitrification has been developed by Jensen *et al.* [2001]. This study investigates the efficiency of denitrification under varying assumptions about temperature, number density, and NAD and NAT relative concentrations. Carslaw *et al.* [2001] simulates the history of the large NAT particles observed by Fahey *et al.* [2001] using isentropic trajectories based on ECMWF meteorological analyses.

3.2.3 Chemistry of the polar vortex

Chlorine and bromine are principally responsible for ozone loss in the polar vortex. The evolution of chlorine activation over the course of the winter was monitored by observations of OClO by the GOME satellite observations [Wagner *et al.*, 2001]. These observations showed strong activation starting around December 22, peaking in mid-February, decreasing steeply in mid-March and ending around March 22. The 1999/2000 winter had the highest activation level of all of the winters observed by GOME since its launch in 1995. Observation of HCl and ClO by ASUR [Bremer *et al.*, 2001] showed relatively high levels of HCl in early December (1st phase), with low HCl and high ClO

in January (2nd phase), consistent with the activation on the extensive PSCs observed by POAM. *In situ* observations of ClO and Cl_2O_2 during the second phase also showed a vortex that was fully activated [Stimpfle *et al.*, 2001]. Satellite observations by MLS showed good agreement with these results [Santee *et al.*, 2001; Danilin *et al.*, 2001].

Microwave ground measurements of ClO profiles at Ny Alesund and Kiruna [Klein *et al.*, 2001; Kopp *et al.*, 2001] also show a highly activated vortex. Simultaneous measurements of BrO and OClO during the LPMA/DOAS flight showed high chlorine activation in mid-February, and these high levels of ClO persisted into the 3rd SOLVE-THESEO 2000 phase [**Klaus Pf to send REF**]. This overall picture is consistent with the ClO observations performed on the TRIPLE gondola which indicate that ClO was highly activated on January 27 and that it was still high on March 1 [Vogel *et al.*, 2001]. Analysis of *in situ* measurements of ClO at sunset on the HALOZ 2 flight on January 27 2000 suggests that the rate of recombination for ClO+ClO -> Cl_2O_2 under cold stratospheric conditions is about 25%-30% faster than currently recommended values [Vömel *et al.*, 2001].

Heterogeneous reactions have been directly observed in numerous laboratory simulations, and these reactions are part of the basis for photochemical models of the stratosphere. Hanisco *et al.* [2001] reports measurements made on the ER-2 that show air being heterogeneously processed inside a polar stratospheric cloud. Large perturbations of HOx observations were found to be consistent with HOCl production via $ClONO_2$+H_2O reaction.

Denitrification of the polar vortex makes much less NO_2 available for reacting with ClO. Thus, denitrification allows ozone loss to persist, since the remaining NO_2 cannot deactivate the ClO catalytic loss process as effectively. Konopka *et al.* [2001] show that mixing of air masses with activated chlorine and air masses with high NOx levels had only a weak influence on chlorine deactivation prior to mid-March. The deactivation is caused mainly by chemistry, i.e. $ClONO_2$ formation with NOx being formed from HNO_3 even in denitrified air masses.

3.2.4 Empirical and modeled calculations of chemical ozone loss

Ozone was a fundamental observation during SOLVE-THESEO 2000. As outlined in section 2.2, satellite, balloon, ground, and aircraft observations of ozone were carried out over the entire winter of 1999/2000. In particular, while the SAGE III satellite was not launched in time for the mission, this satellite instrument will have a similar orbit and measurements as the POAM III satellite instrument. Lumpe *et al.* [2001] compares ozone from POAM with ER-2, MkIV, DOAS, Arotel, DIAL, and

ozone-sondes. This comparison shows reasonably good agreement from the tropopause to the upper stratosphere, and provides confidence in the solar occultation measurements and our ability to monitor ozone with such a platform. Randall *et al.* [2001] uses these POAM observations to construct three dimensional ozone fields using a potential vorticity and potential temperature technique. Danilin *et al.* [2001] presents another comparison technique that uses trajectories to show good agreement between instruments.

Precise ozone loss estimates are critical components to our understanding of stratospheric photochemistry. Theory and modeling have predicted large polar ozone losses under certain conditions in the Arctic. While a number of studies have been shown these losses in the last few years, the loss uncertainties have been large, and there were unresolved assumptions in those loss estimates. Harris *et al.* [2001] discuss the loss estimates for a number of winters, and show generally good agreement between the Match technique, vortex ozone-sonde averages, MLS, HALOE, and REPROBUS (SAOZ, POAM) as long as the comparisons are precise in terms of the temporal and spatial coverage.

A number of papers in this issue and previous publications calculate ozone losses for the 1999/2000 winter. Table 5 lists chemically driven ozone loss estimates derived from the SOLVE-THESEO 2000 campaign for the period from January 20 to March 19 at about 450K isentropic level. This was a period for which many techniques can provide estimates; the losses shown in Table 5 are not losses for the whole winter. The estimates shown in the table show that tremendous ozone loss occurred inside the Arctic polar vortex during the 1999/2000 winter and that there is broad agreement about the rough magnitude of the loss. However these numbers should not be used for a detailed comparison of the loss estimates from the different techniques.

The losses tend to cluster near 1.7 ppmv over this period with variations from 1.0 to 2.3 ppmv. Studies using data from instruments with coarse vertical resolution tend to have lower loss rates (e.g., Bremer *et al.* [2001], Kopp *et al.* [2001], and Klein *et al.* [2001]). The time period of estimate is also a source of differences between analyses. The MSX ozone losses [Swartz *et al.*, 2001] do not include the critical week in mid-March when losses were quite high, while the HALOE study period [Müller *et al.*, 2001] begins in December. The 2.3 ppmv loss derived from MLS data is the product of the 40 ppbv/day loss rate (derived from the first 2 weeks of February) and the 52 day period between January 20 and March 12 with the inclusion of a vertical descent correction of a 5 ppbv/day correction for vertical descent. Additional sources of differences include descent rate differences and averaging technique. When accounted for, the losses show reasonably good consistency and provide great confidence in our ability to quantify ozone loss inside the polar vortex.

These large losses are similar to the ozone losses calculated by models [Sinnhuber et al, 2000] and KASIMA [Kopp *et al.*, 2001], with the ozone loss in the vortex edge region being lower than in the vortex core [Grooß *et al.*, 2001]. Gao *et al.* [2001] show that the ozone loss rate is directly tied to the level of denitrification. They calculated ozone loss rates of 63 ppbv/day at 3-5 ppbv of NO_y and 43 ppbv/day for 7-9 ppbv of NO_y. Davies *et al.* [2001] use the SLIMCAT model to simulate both denitrification and its effect on ozone loss, and they find that a 70% denitrification delays recovery by approximately 10 days. The ClaMS model study of Grooß *et al.* [2001] indicates that the effect of denitrification on ozone depletion starts in early March. In the vortex core (equivalent latitude ≥ 80°N) the additional ozone depletion ascribed to denitrification is 0.13 ppmv (10%) by March 12 and 0.26 ppmv (16%) by March 20.

4.0 Summary

The SOLVE-THESEO 2000 campaign was the largest and most comprehensive study of the polar lower stratosphere that has ever been conducted. The 1999-2000 winter was cold, and the phase timing worked very near perfectly. The first phase occurred during this period of first appearance of temperatures cold enough for PSC formation. The 2nd phase occurred as cold temperatures covered extensive regions of the Arctic. The third phase covered the disappearance of cold temperatures as the vortex began its break up.

The cold temperatures of the Arctic lower stratosphere during the 1999-2000 winter led to the formation of extensive layers of polar stratospheric clouds (PSCs). While PSCs were observed during the December 1st phase, extensive PSCs were encountered during the second phase by the various platforms of SOLVE-THESEO 2000. These PSCs fully processed the air inside the vortex by mid-December. Temperatures tended to remain cold throughout the winter and into mid-March. Again, PSCs were observed by our platforms up to mid-March.

Activated chlorine levels were observed during the second and third phases of SOLVE-THESEO 2000, but were not observed in the first phase. The extensive measurements of chlorine species by a variety of instruments provide the most extensive and precise determination of the evolution of chlorine over the course of a single winter.

Because of the high amounts of ClO_x in the Arctic, and because of the persistence of PSCs into March, there were large chemical ozone losses in the lower stratosphere. Satellite, ozone-sonde, *in*

situ aircraft and balloon, and ground observations reveal that losses exceeded 60% in a layer of the lower stratosphere (460 K).

5.0 Acknowledgements

We would like to thank the pilots and ground crews of all the aircraft that participated in SOLVE-THESEO 2000. In particular, we would like to thank the ER-2 pilots, James Barrilleaux, Jan V. Nystrom, and DeLewis Porter; the DC-8 pilots, Frank Batteas, William Brockett, Richard Ewers, Gordon Fullerton, and Edwin Lewis; the Swiss Air Force pilots, Oberstlt Peter Hauser and Hptm Patrik Steiner; the DLR Falcon pilots, Roland Welser and Peter Vogel; the Mystère 20 pilots; and the ARAT pilots. The NASA aircraft and pilots were magnificently supported by the personnel of NASA's Dryden Flight Research Center Airborne Science Directorate, and we would like to especially thank ER-2 crew chiefs Jim Barnes and Ron Lopez, and DC-8 crew chiefs Steve Davis and Paul Ristrim, as well as their crews. Similarly, a special mention goes to Jeannine Rüetschi and the ground support team at ELTA for the Swiss Air Force Learjet. We also wish to thank the Swiss Air Force for providing their aircraft for this campaign. We are also grateful for the ground support for DLR falcon and CNRS/INSU ARAT and Mystère 20. Finally, we would like thank all the staff at the staff at Kiruna Airport and, specifically, Ulf Mukka for logistical operational support and Tommy Pettersson for his leadership.

The balloon-launching teams of France's CNES and the U. S. National Scientific Balloon Facility (NSBF) spent many long weeks at Esrange waiting patiently and launching efficiently. This contribution was invaluable. We would like to specifically mention and thank Pierre Faucon and his deputies Max Baron, Pierre Dedieu, and Michel Bas for their leadership of the CNES balloon-launching team from Aire sur'Adour and Danny Ball, Dwayne Orr, and Erich Klein were the NSBF Campaign Managers of the NSBF team from Palestine, Texas, USA, and David Shiffrin of the CAO from Moscow for the coordination and recovery of the flights in Russia. The efforts of these visiting launch teams was most enthusiastically and ably complemented by the balloon group at Esrange, and we would particularly like to thank Borje Sjoholm, Tomas Hedquist, and Per Baldeman for their own hard work and for that of the whole launch team. Other members of the Esrange staff also contributed enormously to the success of the campaign; we would like to acknowledge Jan Englund, Stig Kemi, and Alf Wikström for their many and varied contributions, and Johanna Bergstrom-Roos for her help with public relations and the organization of Commissioner Busquin's visit.

Many personnel were involved at ground stations away from the main theatre of operations, but their contributions are no less important. In particular, we would like to thank the individuals responsible for the operation of the ground-based instruments, for launching ozone-sondes at all hours of the day and night, and for the accelerated production of data from satellites.

The NASA Ames Earth Science Project Office made tremendous contributions to the operations and overall success of SOLVE. Our special thanks go to Sue Tolley, Quincy Allison,Wendy Dolci, Steve Gaines, and Joe Goosby.

Overflights of Russian airspace were critical to the success of SOLVE-THESEO 2000. We are especially grateful to General Valery Zakharin and his team for coordinating these over-flights. Special thanks to Academician Nicolai Laverov and Dr. Anatoli Khrenov for facilitating discussions that led to these over-flights.

The European Union provided financial assistance for THESEO 2000 through a number of European and national funding agencies. Acknowledgements for support are given most appropriately in all the individual research papers that are being published. Here we would like to thank DG Research of the European Commission for their overall support for THESEO 2000 through many projects in their Environment and Sustainable Development Programme, and particularly for the coordination of THESEO 2000 through the CASSIS and CRUSOE concerted actions (ENV4-CT97-0550 and EVK2-1999-00252). We would also like to thank the following national funding agencies for their important contributions and apologize to those we have inadvertently omitted: CNES, CNRS-INSU, and the PNCA Programme in France; the BMBF and Max-Planck-Gesellschaft in Germany; the National Environment Research Council and Department of Environment, Transport and the Regions in the UK; CNR and the Italian Space Agency in Italy; the Belgian Offices for Scientific, Technical and Cultural Affairs; the Norwegian Research Council; the Swedish Space Board; ETH in Switzerland; and the Finnish Meteorological Institute.

SOLVE was sponsored by National Aeronautics and Space Administration through its Upper Atmosphere Research Program (UARP), the Atmospheric Effects of Aviation Project (AEAP), the Atmospheric Chemistry Modeling and Analysis Program (ACMAP), and the EOS Validation Program. This sponsorship was performed in cooperation with the National Oceanic and Atmospheric Administration (NOAA), and the National Science Foundation (NSF) and the National Center for Atmospheric Research (NCAR).

We would like to record our special appreciation and thanks to Kathy Wolfe and Rebecca Penkett for their dedication and effort throughout the planning, operation, and post-mission analysis of SOLVE-THESEO 2000. Kathy was most ably assisted by Rose Kendall and Randy Soderholm, to whom we also send our heartfelt thanks.

Finally, we are particularly grateful to the people of Kiruna, Sweden. Their foresight led to the construction of the Arena Arctica, whose location and accommodations were major factors in the success of SOLVE-THESEO 2000. In addition, the hospitality of the citizens of Kiruna made the extended visits of our numerous teams both pleasant and enjoyable.

6.0 Figure Captions

Figure 1. SOLVE-THESEO 2000 operations region. Kiruna, Sweden is noted at the center of the image with the green star. The magenta line indicates a distance of 2700 km from Kiruna. The blue dots indicate ground observation sites, while the red dots indicate ozone-sonde sites. Also superimposed are 50 hPa January average temperature contours (1979-1999). On average, the coldest region of the lower stratosphere is centered on Spitzbergen.

Figure 2. Zonal mean total ozone from the TOMS instrument. The latitude of Kiruna is superimposed as the red line, the occultation latitude of the POAM observations is superimposed as the magenta line, and the sunrise (sunset) occultations of the HALOE instrument are superimposed as the blue crosses (stars).

Figure 3. NASA-ER-2 with payload layout in front of the Arena Arctica in Kiruna, Sweden

Figure 4. NASA DC-8 taking off from Kiruna with its payload layout

Figure 5. DLR Falcon with OLEX lidar.

Figure 6. PSC analysis balloon gondola with attached instruments.

Figure 7. Ozone mixing ratios (ppmv) from ozone-sonde measurements at Ny-Alesund. The broken lower white line indicates the tropopause, the middle white line shows the 380 K isentropic level, and the upper white line represents the 480 K isentropic level. The vertical lines represent the altitude coverage of the DC-8 (white), ER-2 (black), Falcon (orange), ARAT (red), Mystère (green), and Lear Jet (cyan) for their respective flight dates.

Figure 8. Average vortex temperature as a function of potential temperature. Height scale on the right axis is an estimate based upon a 6.5 km scale height. The average is computed over an equivalent latitude range from 75-90°N using the UKMO data at each theta level from 350 to 900K.

The white vertical lines indicate balloon launches and symbols at the top indicate the balloon payload (see Table 4 and the payload section for details).

Figure 9. Mean wind parallel to lines of equivalent latitude on the 600 K isentropic surface (equivalent to a zonal mean in a vortex centered coordinate system).

Figure 10. Potential vorticity on the 450 isentropic surface.

Figure 11. Total ozone averaged between 63-90°N during the month of March for the Northern Hemisphere. Updated from Newman *et al.* [1997].

7.0 Tables

Table 1. Ground Instruments during the SOLVE-THESEO 2000 campaign.

SITE	LAT. °N	LON. °E	INSTRUMENTS	PROFILE	COLUMN
Observatoire Haute Provence, France	43.94	5.71	Lidar, SAOZ, Dobson, O_3 sonde, DOAS	O_3, Aer.	O_3, NO_2, BrO
Plateau de Bure, France	44.63	5.90	microwave	ClO, O_3	
Observatoire de Bordeaux, France	44.83	-0.52	SAOZ, Dobson, microwave, DOAS	O_3	O_3, NO_2, BrO
Jungfraujoch, Switzerland	46.50	8.00	SAOZ, microwave, FTIR	ClO	O_3, NO_2, CO, CH_4, HNO_3, N_2O, $ClONO_2$, HCl, HF
Bern, Switzerland	46.95	7.45	microwave	O_3	
Zugspitze, Germany	47.42	10.98	FTIR		O_3, NO_2, CO, CH_4, HNO_3, N_2O, $ClONO_2$, HCl, HF
Garmisch, Germany	47.48	11.06	Lidar	Aer.	
Cambridge	52.00	0.00	DOAS		BrO
Bremen, Germany	53.00	9.00	DOAS		O_3, NO_2, BrO
Lerwick, UK	60.13	1.18	Dobson, O_3 sonde	O_3	O_3
Harestua, Norway	60.20	10.80	DOAS, FTIR, Dobson	O_3	O_3, NO_2, COF_2, HNO_3, N_2O, OClO, BrO, $ClONO_2$, ClO, HCl, HF
Salekhard, Russia	66.70	66.70	SAOZ		O_3, NO_2
Zhigansk, Russia	67.20	123.40	SAOZ		O_3, NO_2
Sodankyla, Finland	67.37	26.65	Back. sonde, O_3 sonde, SAOZ, Brewer	O_3, Aer.	O_3, NO_2
Kiruna, Sweden	67.84	20.41	DOAS, FTIR, MW,	O_3, N_2O, CH_4, HNO_3, NO, HCl, HF, ClO	O_3, N_2O, CH_4, HNO_3, NO_2, NO, $ClONO_2$, HCl, ClO, COF_2, HF, OClO, BrO
Esrange, Sweden	67.88	21.06	DOAS, lidar, O_3 sonde, radar	Aer., O_3, wind	O_3, NO_2
Andøya, Norway	69.30	16.00	Lidar, O_3 sonde, DOAS	O_3, Aer.	O_3, NO_2, OClO, BrO
Scoresbysund, Greenland	70.48	-21.97	SAOZ		O_3, NO_2
Thule, Greenland	76.53	-68.74	O_3 sonde, DOAS, SAOZ, Back. sonde	O_3, Aer.	O_3, NO_2, OClO
Ny Alesund, Spitsbergen	78.92	11.93	FTIR, SAOZ, Lidar, DOAS, microwave, O_3 sonde, Back. sonde	O_3, Aer., ClO	O_3, NO_2, OClO, BrO, CO, CH_4, HNO_3, N_2O, ClO, HCl, HF

Table 2. ER-2 Payload

Instrument	Investigator	Institution	Measurements
ACATS	J. W. Elkins	NOAA/CMDL	CFC-11, CFC-12, CFC-113, CH_3CCl_3, CCl_4, halon-1211, $CHCl_3$, CH_4, H_2, N_2O, SF_6
ALIAS	C. Webster	JPL	HCl, CO, CH_4, N_2O
Argus	H. Jost	NASA/ARC	N_2O, CH_4
CIMS	P. Wennberg F. Eisele	Cal. Tech. NCAR	HNO_3
$ClONO_2$	R. Stimpfle	Harvard U.	ClO, $ClONO_2$, Cl_2O_2, BrO
CO_2	S. Wofsy	Harvard U.	CO_2
CPFM	C. T. McElroy	AES-Canada	UV-Vis. Spectra, column O_3 J values, Albedo
FCAS N-MASS Impactor	J. Wilson	U. Denver	.07-1 μm particles 4 to 60 nm particles particle composition & structure
H_2O	E. Weinstock R. Spackman	Harvard U.	H_2O
HO_x	T. Hanisco, J. Smith	Harvard U.	OH, HO_2
JLH	R. Herman	JPL	H_2O
MASP	D. Baumgardner B. Gandrud	NCAR	0.4 to 20 μm particles
MMS	T. P. Bui	NASA/ARC	T, P, U, V, W, position
MTP	M. Mahoney	JPL	Temp. profiles
NO_2	K. Perkins E. Lanzendorf	Harvard U.	NO_2
NO_y	D. Fahey, R. Gao	NOAA/AL	NO, NO_y
Ozone	E. Richards	NOAA/AL	O_3
WAS	E. Atlas S. Schauffler	NCAR	CFCs, Halons, HCFCs, N_2O, CH_4, HFCs, PFCs, Hydrocarbons, etc.

Table 3. DC-8 Payload

Instrument	Investigator	Institution	Measurements
LASE	E. Browell	NASA/LARC	H_2O & aerosol back. prof.
UV DIAL	E. Browell	NASA/LARC	O_3 & aerosol prof.
SAFS	R. Shetter	NCAR	Actinic flux 280-535 nm J values
ASUR	K. Kunzi	U. Bremen	Prof. of ClO, HCl, N_2O, O_3, HNO_3, CH_3Cl, H_2O, HO_2, BrO
CIMS	A. Viggiano	AF Research Lab	SO_2, HCN, HNO_3
PMS	B. Anderson	NASA/LARC	0.1-3 μm particles, cn concentrations
O_3	M. Avery	NASA/LARC	O_3
Dew point	J. Barrick	NASA/LARC	Dew Point.
FTIR	W. Mankin	NCAR	Columns of N_2, H_2O, CO_2, CF_2Cl_2, HCN, N_2O, HCl, O_2, HDO, CO, $CFCl_3$, OCS, NO, HF, O_3, CH_4, NO_2, C_2H_6, HNO_3, $ClONO_2$
NO_y	Y. Kondo	U. Tokyo	NO, NO_y
AEROTEL	T. McGee, J. Burris C. Hostetler	NASA/GSFC NASA/LARC	O_3, temp., aerosol prof. Prof. aerosol scattering, backscatter, polarization
Solar Cam	C. Hostetler	NASA/LARC	Solar Images
DACOM	G. Sachse	NASA/LARC	CO, CH_4, N_2O
DLH	G. Sachse, J. Podolske	LARC/Ames	H_2O
NDIR	S. Vay	NASA/LaRC	CO_2
JLH	R. Herman	JPL	H_2O
ATHOS	B. Brune	Penn State	OH, HO_2
ClO/BrO	D. Toohey	U. Colorado	ClO, BrO
TOTCAP	L. Avallone	U. Colorado	O_3, total H_2O, CO_2, F11, F12, F113, Halon-1211, CCl_4
FCAS II NMASS	J. Reeves	U. Denver	0.08 to 2 μm particles 4 to 100 nm particles
MTP	M. Mahoney	JPL	Temp. profiles

Table 4a. Flight Log: phase 1

Date	Platform	Flight time	Min Lat.	Max Lat.	Site	Comment	Max alt.
991109	Descartes				Esrange		
991117	SAOZ Descartes				Andøya		27.0km/14.1 hPa/ 682.4 K
991119	OMS *in situ*				Esrange		30.1km/8.14 hPa/789K
991130	DC-8	9.90	34.87	78.07	Kiruna	Transit	11.3km/216hPa/347K
991202	DC-8	8.36	63.04	79.59	Kiruna	Vortex Survey	11.3km/216hPa/337K
991203	OMS-remote Descartes	6.03			Esrange		33.2km/4.65hPa/960K
991205	DC-8	8.75	61.94	80.70	Kiruna	PSC Survey	11.9km/196hPa/346K
991207	DC-8	9.73	67.81	85.67	Kiruna	PSC Survey	12.5km/178hPa/359K
991210	DC-8	8.53	67.51	82.83	Kiruna	Vortex Survey	12.5km/178hPa/356K
991212	DC-8	9.66	67.67	81.27	Kiruna	PSC Survey	12.5km/178hPa/360K
991214	DC-8	8.33	59.62	69.02	Kiruna	Vortex Survey	12.5km/178hPa/357K
991215	Descartes				Esrange		25.86 km/?/?
991216	DC-8	10.48	34.91	78.18	Kiruna	Transit	11.9km/196hPa/352K

Table 4b. Flight Log: phase 2

Date	Platform	Flight time	Min Lat.	Max Lat.	Site	Comment	Max. alt.
000114	DC-8	10.00	34.88	78.18	Kiruna	Transit	12.5km/178hPa/347K
000114	ER-2	7.30	42.20	71.72	Kiruna	Transit	20.5km/51hPa/484K
000116	DC-8	10.04	60.15	82.00	Kiruna	PSC survey	12.5km/178hPa/366K
000119	HALOZ1, Dirac	?	?	?	Esrange		?/42hPa/482K
000119	PSC-Analysis	13768s			Esrange		17.4 hPa
000119	ARAT				Kiruna	Transit	
000120	DC-8	9.77	62.20	89.35	Kiruna	PSC survey	12.5km/178hPa/347K
000120	ER-2	8.04	65.26	89.11	Kiruna	PSC survey	20.9km/48hPa/463K
000123	DC-8	10.32	58.57	73.77	Kiruna	Vortex sunrise	12.5km/178hPa/343K
000123	ER-2	5.65	58.727	3.86	Kiruna	Vortex sunrise	20.8km/48hPa/466K
000123	Salomon	?	66 (mean)		Esrange		18.2km/59hPa
000124	Falcon	1.53	56.57	67.26	Kiruna	Transit	11.9km/229hPa
000125	DC-8	10.36	59.37	75.89	Kiruna	Mountain waves	12.5km/177hPa/346K
000125	Falcon	2.12	64.73	68.88	Kiruna	Mountain waves	11.9km/229hPa
000125	micro-Radibal				Esrange		21.0km/38hPa/ ?
000125	PSC-Analysis	13044s			Esrange	PSC flight	24.6 hPa
000125	ARAT				Kiruna	PSC analysis	
000126	ARAT				Kiruna	PSC analysis	
000126	Falcon	1.47	62.15	68.18	Kiruna	Mountrain waves	10.7km/267hPa
000127	TRIPLE	16586s			Esrange		25.69km/ 18.94hPa/618K
000127	HALOZ2 Dirac				Esrange		?/35hPa/499K
000127	Falcon	1.33	67.27	68.46	Kiruna	Mountain waves	10.7km/266hPa
000127	ARAT				Kiruna	Transit	
000127	DC-8	9.71	51.48	68.00	Kiruna	Edge survey	12.5km/178hPa/344K
000127	ER-2	6.10	51.52	67.92	Kiruna	Edge survey	21.0km/47hPa/475K
000128	SAOZ SAOZ-BrO, Descartes CH_4 O_3 sensor				Esrange		27km/12.7hPa/ 754K
000129	DC-8	10.78	34.91	78.18	Kiruna	Transit	12.5km/178hPa/368K
000131	ER-2	3.90	67.81	79.05	Kiruna	Vortex survey	20.4km/51hPa/451K
000131	Falcon	2.56	68.98	79.21	Kiruna	NAT-rocks	10.7km/267hPa
000202	ER-2	7.57	64.19	77.86	Kiruna	Vortex survey	20.9km/48hPa/459K
000202	Falcon	2.58	68.24	79.39	Kiruna	NAT-rocks	10.7km/267hPa
000203	ER-2	3.21	67.83	73.16	Kiruna	Multiple level	20.8km/49hPa/458K
000203	Falcon	1.44	68.45	73.39	Kiruna	NAT-rocks	10.7km/266hPa
000204	Falcon	2.28	48.76	66.35	Kiruna	Transit	11.3km/247hPa
000209	SAOZ, SAOZ-BrO, CH_4 O_3 sensor				Esrange		25km/21.4hPa/ 632K
000213	SAOZ, SAOZ-BrO Descartes, CH_4 O_3 sensor				Esrange		26km/17.9hPa/ 729K

In addition, NOAA/CMDL frost-point hygrometers were launched as separate payloads on November 10 (coinciding with OMS), November 14, November 20, November 26, January 25 (after PSC Analysis), January 27 (after Triple and Haloz), March 3, and March 5 (with OMS).

Table 4c. Flight Log: phase 3

Date	Platform	Flight time	Min Lat.	Max Lat.	Site	Comment	Max. alt. Alt/pressure/theta
000218	LPMA/DOAS				Esrange		29.5km
000218	Mir1e				Esrange	2 days	
000218	Mir2e				Esrange	18 days	
000222	Salomon2e				Esrange		29km/11.4hPa/NA
000226	ER-2	7.46	62.93	84.80	Kiruna	Vortex survey	20.5km/50hPa/455K
000227	SAOZ, CH_4, LABS				Esrange	MIR support	24 km/22hPa/632K
000227	DC-8	10.25	34.88	78.18	Kiruna	Transit	12.5km/179hPa/352K
000228	Mystere				Paris		
000229	techno.Mir3				Esrange		
000301	TRIPLE				Esrange		NA/21.7hPa/NA
000301	HALOZ3Desca rts				Esrange		18.1km/57hPa
000303	DC-8	9.99	60.69	86.53	Kiruna	Vortex edge	12.5km/178hPa/338K
000305	DC-8	9.55	63.82	79.37	Kiruna	Vortex survey	12.5km/178hPa/337K
000305	ER-2	7.85	66.68	81.04	Kiruna	Vortex survey	20.8km/48hPa/467K
000305	OMS *in situ*, Dirac Descartes				Esrange		29.3km/8.89hPa/845K
000307	SAOZ, SAOZ-BrO Labs, Descartes				Esrange		27km/9.7hPa/820K
000307	Mystere				Paris		
000307	ER-2	7.90	67.83	82.96	Kiruna	Vortex survey	20.8km/48hPa/467K
000308	DC-8	10.67	63.10	80.25	Kiruna	PSC survey	12.5km/178hPa/336K
000308	HALOZ4, Dirac				Esrange		?/46hPa/475K
000308	Learjet				Kiruna	Transit	
000309	DC-8	9.92	57.40	80.14	Kiruna		12.5km/178hPa/346K
000309	Learjet				Kiruna	Iceland flight	
000310	Learjet				Kiruna	North Pole	
000311	Learjet				Kiruna	Arctic Sea	
000311	DC-8	8.78	67.58	80.09	Kiruna	Vortex edge	12.5km/178hPa/342K
000311	ER-2	7.97	58.60	75.08	Kiruna	Vortex edge	20.9km/47hPa/474K
000312	ER-2	7.44	65.27	79.46	Kiruna	Vortex survey	20.6km/50hPa/466K
000313	DC-8	8.66	65.07	83.91	Kiruna	Vortex survey	12.5km/178hPa/354K
000313	Learjet				Kiruna	Transit	
000315	DC-8	8.77	46.95	86.33	Kiruna	Transit	11.3km/216hPa/349K
000315	OMS remote	5.01			Esrange		29.1km/11.3hPa/850K
000316	ER-2	9.02	42.21	67.81	Kiruna	Transit	20.4km/51hPa/508K
000325	SAOZ, BrO. Dirac CH_4				Esrange		28km/12.3hPa/837K
000326	Mystere				Paris		
000328	Mystere				Paris		
000403	SAOZ, Descartes				Andøya		26km/11.9hPa/822K
000404	HALOZ5 Descartes				Esrange		15.32km/103hPa/407K

Table 4. SOLVE-THESEO 2000 flight log for all 3 phases.

Table 5. Ozone Loss Rates

Polar Vortex Ozone Loss at 450 K on Mar. 12 (estimated from observations between Jan. 20 and Mar. 12, 2000)			
Paper	**O_3 Loss (ppmv)**	**Uncertainty (ppmv)**	**Data Set**
Bremer *et al.* [2001]	[A]1.05	±0.1	ASUR
Grant *et al.* [2001]	1.5	±0.3	LARC DIAL
Hoppel *et al.* [2001]	1.45	±0.2	POAM III solar occultation
Klein *et al.* [2001]	[A]0.7	±0.3	Ny Ålesund microwave radiometer
Kopp *et al.* [2001]	[A]1.1	±0.2	Kiruna FTIR O_3, N_2O, HF
	1.4	±0.6	microwave O_3, FTIR N_2O, HF
Lait *et al.* [2001]	1.7	±0.3	PV-θ analysis - Ozone-sondes
Müller *et al.* [2001]	[B]2.2	±0.3	HALOE and OMS
Rex *et al.* [2001]	1.7	±0.2	Match - Ozone-sondes
Richard *et al.* [2001]	1.8	±0.3	ER-2 tracer-tracer
Robinson *et al.* [2001]	[C]1.35	±0.12	Dirac tracer-tracer
	[D]1.10	±0.1	Descartes tracer-tracer
Salawitch *et al.* [2001]	[E]1.36	±0.21	OMS measurements
	1.76	±0.21	OMS balloon and ER-2 data
Santee *et al.* [2000]	[F]2.3	±0.6	UARS MLS
Schoeberl *et al.* [2001]	1.63	±0.3	Vortex avg. –Ozone-sondes
	1.3	±0.1	POAM III
	1.54	±0.15	Forward trajectory
Sinnhuber *et al.* [2000]	1.7	±0.2	Ny Ålesund ozone-sonde, SLIMCAT model
Swartz *et al.* [2001]	[G]1.0	±0.08	MSX stellar occultation

All losses are corrected for descent unless otherwise noted.

[A] Microwave and IR instruments have ~10 km vertical resolution at 20km altitude.

[B] Estimated between Nov. 1999 and March 11-14, 2001

[C] Estimated between Jan. 23 to March 7

[D] Estimated between Nov. 1999 and March 4, 2001

[E] Estimated for 1/20 to 3/5/2000

[F] Loss rate (0.04 ppmv/day) estimated at 465 K between 2/2 and 2/13/2000 scaled for 52 days, with a 0.25 ppmv correction for downward advection

[G] Estimate based upon ozone change between January 23 and March 4.

8.0 References

Barath, F. T., M. C. Chavez, R. E. Cofield, D. A. Flower, M. A. Frerking, M. B. Gram, W. M. Harris, J. R. Holden, R. F. Jarnot, W. G. Kloezeman, G. J. Klose, G. K. Lau, M. S. Loo, B. J. Maddison, R. J. Mattauch, R. P. McKinney, G. E. Peckham, H. M. Pickett, G. Siebes, F. S. Soltis, R. A. Suttie, J. A. Tarsala, J. W. Waters, and W. J. Wilson, The Upper Atmosphere Research Satellite Microwave Limb Sounder instrument, *J. Geophys. Res., 98*, 10751-10762, 1993.

Becker G, R. Müller R, D.S. McKenna, M. Rex, K.S. Carslaw and H. Oelhaf, Ozone loss rates in the Arctic stratosphere in the winter 1994/1995: Model simulations underestimate results of the Match analysis, *J. Geophys. Res.*, 105, 15175-15184, 2000.

Bevilacqua, R.M., M.D. Fromm, J.M. Alfred, J.H. Hornstein, G.E. Nedoluha,K. W. Hoppel, J.D. Lumpe, and C.E. Randall, Observations and analysis of PSCs detected by POAM III during the 1999/2000 northern hemisphere winter, submitted to *J. Geophys. Res.*, 2001.

Bremer, H., M.V. König, A. Kleinböhl, H. Küllmann, K. Künzi, K. Bramstedt,J. P. Burrows, K.-U. Eichmann, and M. Weber, Ozone depletion observed by ASUR during the Arctic Winter 1999/2000, submitted to *J. Geophys. Res.*, 2001.

Burrows, J.P., M. Weber, M. Buchwitz, V.V. Rozanov, A. Ladstätter-Weißenmayer, A. Richter, R. DeBeek, R. Hoogen, K. Bramstedt and K.U. Eichmann 1999, "The Global Ozone Monitoring Experiment (GOME): Mission Concept and First Scientific Results", Journal of Atmospheric Sciences 56 151-175.

Carslaw, K.S., M. Wirth, A. Tsias, B.P. Luo, A. Dörnbrack, M. Leutbecher, H. Volkert, W. Renger, J.T. Bacmeister and Th. Peter, Particle microphysics and chemistry in remotely observed mountain polar stratospheric clouds, J. Geophys. Res., 103, 5785-5796, 1998.

Carslaw, K. S., J. Kettleborough, M. Northway, S. Davies, R.-S. Gao, D. W. Fahey, D. Baumgardner, M. P. Chipperfield, and A. Kleinböhl, A vortex-scale simulation of the growth and sedimentation of large nitric acid particles observed during SOLVE-THESEO 2000, submitted to *J. Geophys. Res.*, 2001.

Cunnold, D.M., J.M. Zawodny, W.P. Chu, J.P. Pommereau, F. Goutail, J. Lenoble, M.P. McCormick, R.E. Veiga, D. Murcray, N. Iwagami, K. Shibasaki, P.C. Simon, and W. Peetermans, Validation of SAGE II NO_2 Measurements, J. Geophys. Res., 96, 12913-12925, 1991.

Danilin, M.Y., M.K.W. Ko, R.M. Bevilacqua, L.V. Lyjak, L. Froidevaux, M.L. Santee, J.M. Zawodny, K.W. Hoppel, E.C. Richard, J.R. Spackman, E.M. Weinstock, R.L. Herman, K.A. McKinney, P.O. Wennberg, F.L. Eisele, R.M. Stimpfle, C.J. Scott, J.W. Elkins, and T.V. Bui, Comparison of ER-2 Aircraft and POAM-III, MLS, and SAGE-II Satellite Measurements during SOLVE Using Traditional Correlative Analysis and Trajectory Hunting Technique, submitted to *J. Geophys. Res.*, 2001.

Davies, S., M.P. Chipperfield, K.S. Carslaw, B.-M. Sinnhuber, J.G. Anderson, R. Stimpfle, D. Wilmouth, D.W. Fahey, P.J. Popp, E.C. Richard, P. von der Gathen, H. Jost, and C.R.. Webster, Modeling the Effect of Denitrification on Arctic Ozone Depletion During Winter 1999/2000, submitted to *J. Geophys. Res.*, 2001.

Dörnbrack, T. Birner, A. Fix, H. Flentje, A. Meister, H. Schmid, E.V. Browell, and M.J. Mahoney, Evidence for inertia-gravity waves forming polar stratospheric clouds over Scandinavia, submitted to *J. Geophys. Res.*, 2001.

Fahey, D.W., R.S. Gao, K.S. Carslaw, J. Kettleborough, P.J. Popp, M.J. Northway, J.C. Holecek, S.C. Ciciora, R.J. McLaughlin, T.L. Thompson, R.H. Winkler, D.G. Baumgardner, B. Gandrud, P.O. Wennberg, S. Dhaniyala, K. McKinney, Th. Peter, R.J. Salawitch, T.P. Bui, J.W. Elkins, C.R. Webster, E.L. Atlas, H. Jost, J.C. Wilson, R.L. Herman, A. Kleinböhl, and M. V. König, The Detection of Large HNO_3-Containing Particles in the Winter Arctic Stratosphere, *Science*, 291, 1026-1031, 2001.

Farman, J.C., B.G. Gardiner and J.D. Shanklin, Large losses of total ozone in Antarctica reveal seasonal ClO_x/NO_x interaction, *Nature*, 315, 207-210, 1985.

Gao, R.S., E.C. Richard, P.J. Popp, G.C. Toon, D.F. Hurst, P.A. Newman, J.C. Holecek, M.J. Northway, D.W. Fahey, M.Y. Danilin, B. Sen, K. Aikin, P.A. Romashkin, J.W. Elkins, C.R. Webster, S.M. Schauffler, J.B. Greenblatt, C.T. McElroy, L.R. Lait, T.P. Bui, and D.Baumgardner, Observational evidence for the role of denitrification in Arctic stratospheric ozone loss, submitted to *J. Geophys. Res.*, 2001.

Godin, S., M. Marchand, and A. Hauchecorne, Influence of Arctic polar ozone depletion on the lower stratospheric ozone amounts at Haute-Provence Observatory (44°N, 6°E), submitted to *J. Geophys. Res.*, 2001.

Grant, W.B., E.V. Browell, C.F. Butler, S.C. Gibson, S.A. Kooi, and P. von der Gathen, Use of ozone distributions, potential vorticity, and cooling rates to estimate Arctic polar vortex ozone loss during the winter of 1999/2000, submitted to *J. Geophys. Res.*, 2001.

Greenblatt, J.B., H.-J. Jost, M. Loewenstein, J.R. Podolske, T.P. Bui, D.F. Hurst, J.W. Elkins, R.L. Herman, C.R. Webster, S.M. Schauffler, E.L. Atlas, P.A. Newman, L.R. Lait, M. Muller, A. Engel, and U. Schmidt, Defining the polar vortex edge using an N_2O: potential temperature correlation vs. the Nash criterion: A comparison, submitted to *J. Geophys. Res.*, 2001.

Grooß, J.-U., G. Gunther, P. Konopka, R. Müller, D. S. McKenna, F. Stroh, B. Vogel, A. Engel, M. Müller, K. Hoppel, R. Bevilacqua, E. Richard, C.R. Webster, J.W. Elkins, D.F. Hurst, P.A. Romashkin, and D.G. Baumgardner, Simulation of ozone depletion in spring 2000 with the Chemical Lagrangian Model of the Stratosphere (ClaMS), submitted to *J. Geophys. Res.*, 2001.

Hanisco, T.F., J.B. Smith, R.M. Stimpfle, D.M. Wilmouth, K.K. Perkins, J.R. Spackman, J.G. Anderson, D. Baumgardner, B. Gandrud, C.R. Webster, S. Dhaniyala, K.A. McKinney, and T.P. Bui, Quantifying the rate of heterogeneous processing in the Arctic polar vortex with *in situ* observations of OH, submitted to *J. Geophys. Res.*, 2001.

Harris, N.R.P., M. Guirlet, P.A. Newman and A. Adriani, Report on the SOLVE-THESEO 2000 science meeting, SPARC newsletter no. 16, 27-29, 2001

Harris, N.R.P., M. Rex, F. Goutail, B.M. Knudsen, G.L. Manney, R. Müller, and P. von der Gathen, Comparison of Empirically Derived Ozone Losses in the Arctic Vortex, submitted to *J. Geophys. Res.*, 2001.

Hauchecorne, A., S. Godin, M. Marchand, B. Heese, and C. Souprayen, Quantification of the Transport of Chemical Constituents from the Polar Vortex to Middle Latitudes in the Lower Stratosphere using the High-Resolution Advection Model MIMOSA and Effective Diffusivity, submitted to *J. Geophys. Res.*, 2001.

Herman, R.L., K. Drdla, J.R. Spackman, D.F. Hurst, C.R. Webster, J.W. Elkins, E.M. Weinstock, B.W. Gandrud, G.C. Toon, M.R. Schoeberl, H. Jost, E.L. Atlas, P.J. Popp, and T.P. Bui, Hydration, dehydration, and the total hydrogen budget of the 1999-2000 winter Arctic stratosphere, submitted to *J. Geophys. Res.*, 2001.

Hervig, M.E., J.M. Russell III, L.L. Gordley, J.H. Park, S.R. Drayson, and T. Deshler: Validation of Aerosol Measurements from the Halogen Occultation Experiment, J. Geophys. Res., 101, 10,267-10,275, 1996.

Hood, L.L, B.E. Soukharev, M. Fromm and J.P. McCormack, Origin of extreme ozone minima at middle to high northern latitudes, J. Geophys. Res., in press, 2001.

Hoppel, K., R. Bevilacqua, G. Nedoluha, C. Deniel, F. Lefèvre, J. Lumpe, M. Fromm, C. Randall, J. Rosenfield, and M. Rex, POAM III Observations of Arctic Ozone Loss for the 1999/2000 Winter, submitted to *J. Geophys. Res.*, 2001.

Hurst, D.F., S.M. Schauffler, J.B. Greenblatt, H. Jost, R.L. Herman, J.W. Elkins, P.A. Romashkin, E.L. Atlas, S.G. Donnelly, J.R. Podolske, M. Loewenstein, C.R. Webster, G.. Flesch, and D.C. Scott, The Construction of a Unified, High-Resolution Nitrous Oxide Data Set for ER-2 Flights During SOLVE, submitted to *J. Geophys. Res.*, 2001.

James, P. M., A climatology of ozone mini-holes over the northern hemisphere, *Intl. J. of Climo., 18*, 1287-1303, 1998.

Jarnot, R. F., R. E. Cofield, J. W. Waters, D. A. Flower, G. E. Peckham, Calibration of the microwave limb sounder on the Upper Atmosphere Research Satellite, *J. Geophys. Res., 101*, 9957-9982, 1996

Jensen, E.J., O.B. Toon, A. Tabazadeh, and K. Drdla, Impact of Polar Stratospheric Cloud Particle Composition, Number Density, and Lifetime on Denitrification, submitted to *J. Geophys. Res.*, 2001.

Kilbane-Dawe, I., N.R.P. Harris, J.A. Pyle, M. Rex, A.M. Lee and M.P. Chipperfield, A comparison of Match and 3D model ozone loss rates in the Arctic polar vortex during the winters of 1994/95 and 1995/96, *J. Atmos. Chem.*, 39, 123-138, 2001.

Klein, U., I. Wohltmann, K. Lindner, and K. F. Künzi, Ozone Depletion and Chlorine Activation in the Arctic Winter 1999/2000 observed in Ny-Alesund, submitted to *J. Geophys. Res.*, 2001.

Kleinböhl, A., Th. Blumenstock, H. Bremer, E.V. Browell, S. Davies, B. Galle, A.P.H. Goede, W.B. Grant, M. von König, H. Küllman, K.F. Künzi, B-M. Sinnhuber and G. Toon, Vortexwide Denitrification of the Arctic Polar Stratosphere in Winter 1999/2000 determined by Remote Observations, submitted to *J. Geophys. Res.*, 2001.

Konopka *et al.*, sub to JGR, 2001.

Kopp, G., H. Berg, Th. Blumenstock, H. Fischer, F. Hase, G. Hochschild, Y. Kondo, W. Kouker, I. Langbein, U. Raffalski, Th. Reddmann, and R. Ruhnke, Evolution of ozone and ozone related species over Kiruna during the THESEO\2000-SOLVE campaign retrieved from ground-based millimeter wave and infrared observations and modeled with KASIMA, submitted to *J. Geophys. Res.*, 2001.

Lait, L.R., An alternative form for potential vorticity, J. Atmos. Sci., 51, 1754-1759,1994

Lait, L.R., M.R. Schoeberl, P.A. Newman, T. McGee, J. Burris, E.V. Browell, E. Richard, G.O. Braathen, B.R. Bojkov, F. Goutail, P. von der Gathen, E. Kyrö, G. Vaughan, H. Kelder, S. Kirkwood,

P. Woods, V. Dorokhov, I. Zaitcev, Z. Litynska, A. Benesova, P. Skrivankova, H. De Backer, J. Davies, T. Jorgensen, and I. S. Mikkelsen, Ozone Loss from Quasi-Conservative Coordinate Mapping during the 1999-2000 SOLVE Campaign, submitted to *J. Geophys. Res.*, 2001.

N. Larsen, S. Høyer Svendsen, B.M. Knudsen, C. Voigt, A. Kohlmann, J. Schreiner, K. Mauersberger, T. Deshler, C. Kröger, J.M. Rosen, N.T. Kjome, A. Adriani, F. Cairo, G. Di Donfrancesco, J. Ovarlez, H. Ovarlez, A. Dörnbrack and T. Birner, Microphysical mesoscale simulations of polar stratospheric cloud formation over Northern Scandinavia on 25 January 2000 constrained by *in situ* measurements of chemical and optical cloud properties, submitted to *J. Geophys. Res.*, 2001.

Lumpe, J.D., M. Fromm, K. Hoppel, R.M. Bevilacqua, C.E. Randall, E.V. Browell, W.B. Grant, T. McGee, J. Burris, L. Twigg, E.C. Richard, G.C. Toon, B. Sen, H. Boesch, R. Fitzenberger, and K. Pfeilsticker, Comparison of POAM III ozone measurements with correlative aircraft and balloon data during SOLVE, submitted to *J. Geophys. Res.*, 2001.

Lucke R.L., D.R. Korwan, R.M. Bevilacqua, J.S. Hornstein, E.P. Shettle, D.T. Chen, M. Daehler, J.D. Lumpe, M.D. Fromm, D. Debrestian, B. Neff, M. Squire, G. Konig-Langlo, and J. Davies, The Polar Ozone and Aerosol Measurement (POAM) III Instrument and Early Validation Results, *J. Geophys. Res.*, 104, 18785-19799, 1999.

Luo, B.P., Th. Peter, S.A. Füglistaler, H. Wernli, R.-M. Hu, K.S. Carslaw, C.A. Hostetler, L.R. Poole, T.J. McGee, and J.F. Burris, Large Stratospheric Particles Observed by Lidar During SOLVE-THESEO 2000 Mission, submitted to *J. Geophys. Res.*, 2001.

Manney, G.L., and J.L. Sabutis, Development of the polar vortex in the 1999-2000 Arctic winter stratosphere, *Geophys. Res. Lett.*, 27, 2589-2592, 2000.

McCormick, M.P., P. Hamill, T.J. Pepin, W.P. Chu, T.J. Swissler, and L.R. McMaster, Satellite studies of the stratospheric aerosol, Bull. Am. Meteorol. Soc., 60, 1038-1046, 1979.

Meilinger, S.K., T. Koop, B.P. Luo, T. Huthwelker, K.S. Carslaw, U. Krieger, P.J. Crutzen and Th. Peter, Size-dependent stratospheric droplet composition in mesoscale temperature fluctuations and their potential role in PSC freezing, Geophys. Res. Lett., 22, 3031-3034, 1995.

Moore, F.L., J.W. Elkins, E.A. Ray, G.S. Dutton, R.E. Dunn, D. Fahey, R.J. McLaughlin, T.L. Thompson, P.A. Romashkin, D.F. Hurst, and P.R. Wamsley, Balloon-borne in situ gas chromatograph for measurements in the troposphere and stratosphere, submitted to *J. Geophys. Res.*, 2001.

Müller *et al.*, 2001.

Newman *et al.*, 1997.

Newman, SPARC, 2000

Newman *et al.*, 2001

Orsolini, Y.J. and V. Limpasuvan, The North Atlantic Oscillation and the occurrences of ozone miniholes, Geophys. Res. Lett., in press, 2001.

Ovarlez, J., and H. Ovarlez, Water vapour and aerosol measurements during SESAME and the observation of low water vapour content layers, *Air Pollution report N°56*, Polar Stratospheric Ozone, CEC Publ., 205-208, 1995.

Piani, C., W.A. Norton, A.M. Iwi, E.A. Ray, and J.W. Elkins, Transport of Ozone Depleted Air on Breakup of the Stratospheric Polar Vortex in Spring/Summer 2000, submitted to *J. Geophys. Res.*, 2001.

Popp, P.J., M.J. Northway, J.C. Holecek, R.S. Gao, D.W. Fahey, J.W. Elkins, D.F. Hurst, P.A. Romashkin, G.C. Toon, B. Sen, S.M. Schauffler, R.J. Salawitch, C.R. Webster, R.L. Herman, H. Jost, T.P. Bui, P.A. Newman, and L.R. Lait, Severe and Extensive Denitrification in the 1999-2000 Arctic Winter Stratosphere, submitted to *J. Geophys. Res.*, 2001.

Randall, C.E., J.D. Lumpe, R.M. Bevilacqua, K.W. Hoppel, M.D. Fromm, R.J. Salawitch, W.H. Swartz, S.A. Lloyd, E. Kyrö, P. von der Gathen, H. Claude, J. Davies, H. De Backer, H. Dier, I.B. Mikkelsen, M.J. Molyneux, and J. Sancho, Construction of 3D Ozone Fields Using POAM III During SOLVE, submitted to *J. Geophys. Res.*, 2001.

Reichardt, J., S. Reichardt, P. Yang, and T.J. McGee, Retrieval of Polar Stratospheric Cloud Microphysical Properties From Lidar Measurements: Dependence on Particle Shape Assumptions, submitted to *J. Geophys. Res.*, 2001.

Rex, M., R.J. Salawitch, N.R.P. Harris, P. von der Gathen, G.O. Braathen, A. Schulz, H. Deckelman, M. Chipperfield, B.-M. Sinnhuber, E. Reimer, R. Alfier, R. Bevilacqua, K. Hoppel, M. Fromm, J. Lumpe, H. Küllmann, A. Kleinböhl, H. Bremer, M. von König, K. Künzi, D. Toohey, H. Vömel, E. Richard, K. Aikin, H. Jost, J.B. Greenblatt, M. Loewenstein, J.R. Podolske, C.R. Webster, G.J. Flesch, D.C. Scott, R.L. Herman, J.W. Elkins, E.A. Ray, F.L. Moore, D.F. Hurst, P. Romashkin, G.C. Toon, B. Sen, J.J. Margitan, P. Wennberg R. Neuber, M. Allart, B.R. Bojkov, H. Claude, J. Davies, W. Davies, H. De Backer, H. Dier, V. Dorokhov, H. Fast, Y. Kondo, E. Kyrö, Z. Litynska, I.S. Mikkelsen, M.J. Molyneux, E. Moran, T. Nagai, H. Nakane, C. Parrondo, F. Ravegnani, P. Skrivankova, P. Viatte, and V. Yushkov, Chemical depletion of Arctic ozone in winter 1999/2000, *J. Geophys. Res.*, in press, 2001.

Rex, M., P. von der Gathen, G.O. Braathen, N.R.P. Harris, E. Reimer, A. Beck, R. Alfier, R. Krüger-Carstensen, M. Chipperfield, H. De Backer, D. Balis, F. O'Connor, H. Dier, V. Dorokhov, H. Fast, A. Gamma, M. Gil, E. Kyrö, Z. Litynska, I.S. Mikkelsen, M.J. Molyneux, G. Murphy, S.J. Reid, M. Rummukainen, and C. Zerefos, Chemical ozone loss in the Arctic winter 1994/95 as determined by the Match technique, *J. of Atmos. Chem., 32*, 35-59, 1999

Richard, E.C., K.. Aikin, A.E. Andrews, B.C. Daube, Jr., C.Gerbig, S.C. Wofsy, P.A. Romanshkin, D.F. Hurst, E.A. Ray, F.L. Moore, J.W. Elkins, T. Deshler, and G.C. Toon, Severe Chemical Ozone Loss Inside the Arctic Polar Vortex during Winter 1999-2000 Inferred from in situ Airborne measurements, *Geophys. Res. Lett.*, 28, 2197-2200, 2001.

Russell III, J.M., L.L. Gordley, J.H. Park, S.R. Drayson, W.D. Hesketh, R.J. Cicerone, A.F. Tuck, J.E. Frederick, J.E. Harries, and P.J. Crutzen, The Halogen Occultation Experiment, *J. Geophys. Res.*, 98, 10777-10798, 1993.

Salawitch, R.J., J.J. Margitan, B. Sen, G.C. Toon, G.B. Osterman, M. Rex, J.W. Elkins, E.A. Ray, F.L. Moore, D.F. Hurst, P.A. Romashkin, R.M. Bevilacqua, K.Hoppel, E.C. Richard, and T.P. Bui, Chemical Loss of Ozone During the Arctic Winter of 1999-2000: An Analysis Based on Balloon-borne Observations, submitted to *J. Geophys. Res.*, 2001.

Santee, M.L., G.L. Manney, N. J.Livesey, and J.W. Waters, UARS Microwave Limb Sounder Observations of Denitrification and Ozone Loss in the 2000 Arctic Late Winter, *Geophys. Res. Lett.*, 27, 3213-3216, 2000.

Schiller, C., A. Hofzumahaus, M. Müller, E. Klein, E.-P. Röth and U. Schmidt, Ultraviolet actinic flux in the stratosphere: an overview of balloon-borne measurements during EASOE, 1991/92. *Geophys. Res. Lett., 21,* 1239-1242, 1994.

Schiller, C., R. Bauer, F. Cairo, T. Deshler, A. Dörnbrack, J. Elkins, A. Engel, H. Flentje, N. Larsen, I. Levin, M. Müller, S. Oltmans, H. Ovarlez, J. Ovarlez, J. Schreiner, F. Stroh, C. Voigt, and H. Vömel, Dehydration in the arctic stratosphere during the THESE0-2000/SOLVE campaigns, submitted to *J. Geophys. Res.*, 2001.

Schoeberl, M.A., P.A. Newman, L.R. Lait, T.J. McGee, J.F. Burris, E.V. Browell, W.B. Grant, E.C. Richard, P. von der Gathen, R. Bevilacqua, I.S. Mikkelsen, and M.J. Molyneux, An Assessment of the Ozone Loss During the 1999-2000 SOLVE-THESEO 2000 Arctic Campaign, submitted to *J. Geophys. Res.*, 2001.

Schreiner, J., C. Voigt, A. Kohlmann, K. Mauersberger, T. Deshler, C. Kroger, N. Larsen, A. Adriani, F. Cairo, G. Di Donfrancesco, J. Ovarlez, H. Ovarlez, A. Dörnbrack, J. Rosen, and N. Kjome, Chemical, microphysical and optical properties of polar stratospheric clouds, submitted to *J. Geophys. Res.*, 2001.

Sinnhuber, B.-M., M.P. Chipperfield, S. Davies, J.P. Burrows, K.-U. Eichmann, M. Weber, P. von der Gathen, M. Guirlet, G.A. Cahill, A.M. Lee, and J.A. Pyle, Large loss of total ozone during the Arctic winter 1999/2000, *Geophys. Res. Lett.*, 27, 3473-3476, 2000.

Stimpfle *et al.*, 2001

Strawa, A.W., K. Drdla, M. Fromm, R.F. Pueschel, K.W. Hoppel, E.V. Browell, C.A. Hostetler, and P. Hamill, Discriminating Type Ia and Ib Polar Stratospheric Clouds in POAM Satellite Data, submitted to *J. Geophys. Res.*, 2001.

Swartz, W.H., J.-H. Yee, R.J. Vervack, Jr., S.A. Lloyd and P.A. Newman, Photochemical ozone loss in the Arctic as determined by MSX/UVISI stellar occultation observations during the 1999-2000 winter, submitted to *J. Geophys. Res.*, 2001.

Tsias, A., A.J. Prenni, K.S. Carslaw, T.P. Onasch, B.P. Luo, M.A. Tolbert and Th. Peter, Freezing of polar stratospheric clouds in orographically induced strong warming events, *Geophys. Res. Lett.*, 24, 2303-2306, 1997.

Vogel, B., F. Stroh, J.-U. Grooß, R. Müller, D.S. McKenna, M. Müller, T. Deshler, D. Toohey, G. Toon, J. Ovarlez, J. Karhu and A. Dörnbrack, Photo-chemistry of ClO in the Arctic vortex in January and March 2000: In-situ observations and model simulations, submitted to *J. Geophys. Res.,* 2001.

Voigt, C., J. Schreiner, A. Kohlmann, P. Zink, K. Mauersberger, N. Larsen, T. Deshler, C. Kroger, J. Rosen, A. Adriani, F. Cairo, G. Di Donfrancesco, M. Viterbini, J. Ovarlez, H. Ovarlez, C. David, and A. Dörnbrack, Nitric Acid Trihydrate (NAT) in Polar Stratospheric Clouds, *Science*, 2000.

Vömel, H., D. Toohey, and T. Deshler Sunset observations of ClO in the arctic polar vortex and implications for Cl2O2 formation and ozone loss, *Geophys. Res. Lett.*, submitted, 2001.

von König, M., H. Bremer, E.V. Browell, J. Burris, A.P.H. Goede, W.B. Grant, A. Kleinböhl, H. Küllman, K.F. Künzi, T. McGee, and L. Twigg, Using gas-phase nitric acid as an indicator of PSC composition, submitted to *J. Geophys. Res.*, 2001.

Wagner, T., F. Wittrock, A. Richter, M. Wenig, J. P. Burrows, and U. Platt, Continuous monitoring of the high and persistent chlorine activation during the Arctic winter 1999/2000 by the GOME instrument on ERS-2, submitted to *J. Geophys. Res.*, 2001.

Waters, J.W., "Microwave Limb Sounding," in Atmospheric Remote Sensing by Microwave Radiometry, (M.A. Janssen ed.), chapter 8, New York: John Wiley (1993)

Waters, J.W., *et al.*, "The UARS and EOS MLS Microwave Limb Sounder (MLS) Experiments," J. Atmos. Sci. 56, 194-218, 1999.

Waugh, D. W., and Ping-Ping Rong, Interannual Variability in the Decay of Lower Stratospheric Arctic Vortices, submitted to *J. Meteor. Soc.*, 2001.

Zöger, M., A. Afchine, N. Eicke, M.-T. Gerhards, E. Klein, D.S. McKenna, U. Mörschel, U. Schmidt, V. Tan, F. Tuitjer, T. Woyke and C. Schiller, Fast *in situ* stratospheric hygrometers: A new family of balloon borne and airborne Lyman-alpha photofragment fluorescence hygrometers, *J. Geophys. Res., 104*, 1807-1816, 1999.

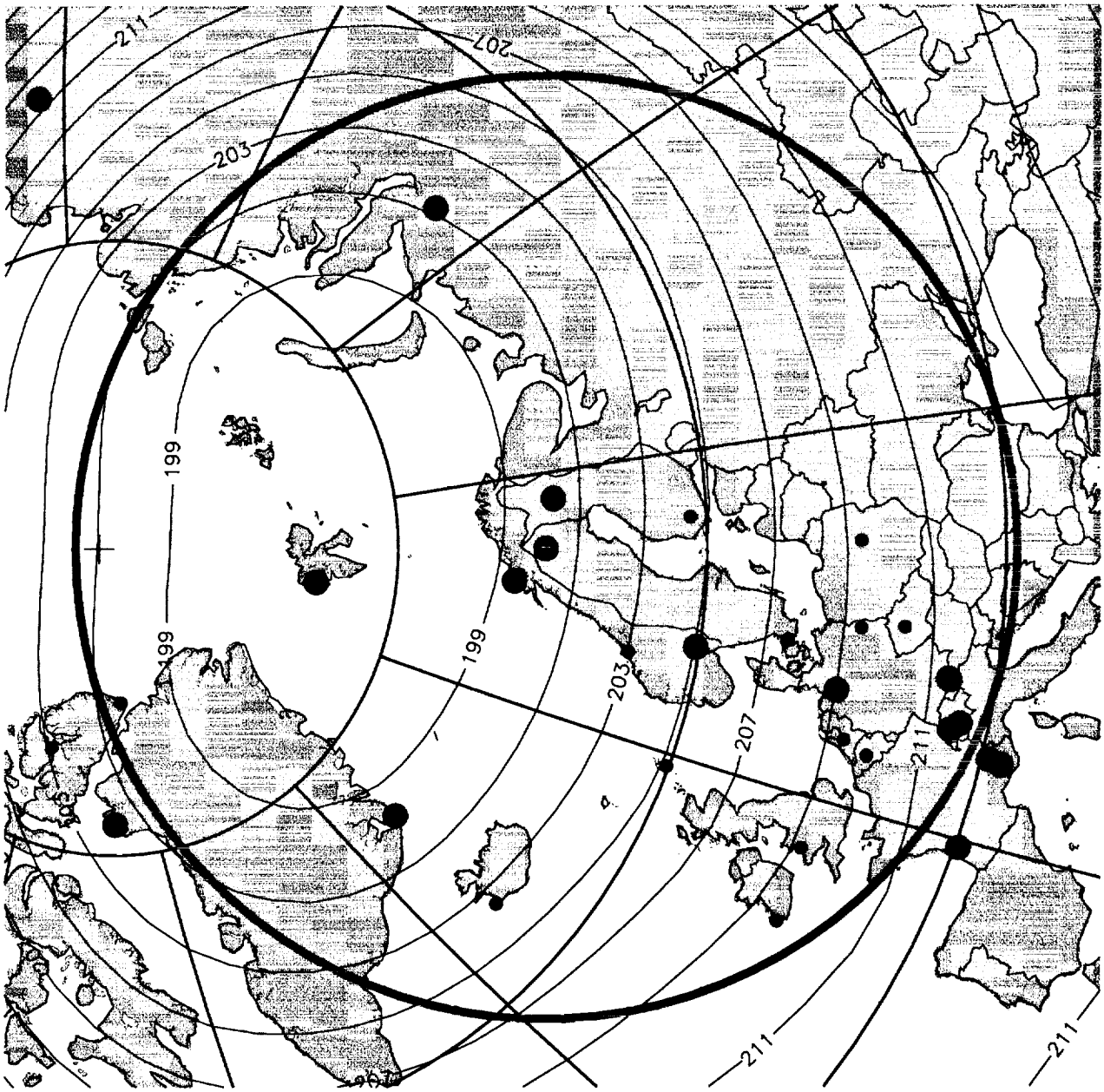
211
207
203
199
199
199
203
207
211
211
211

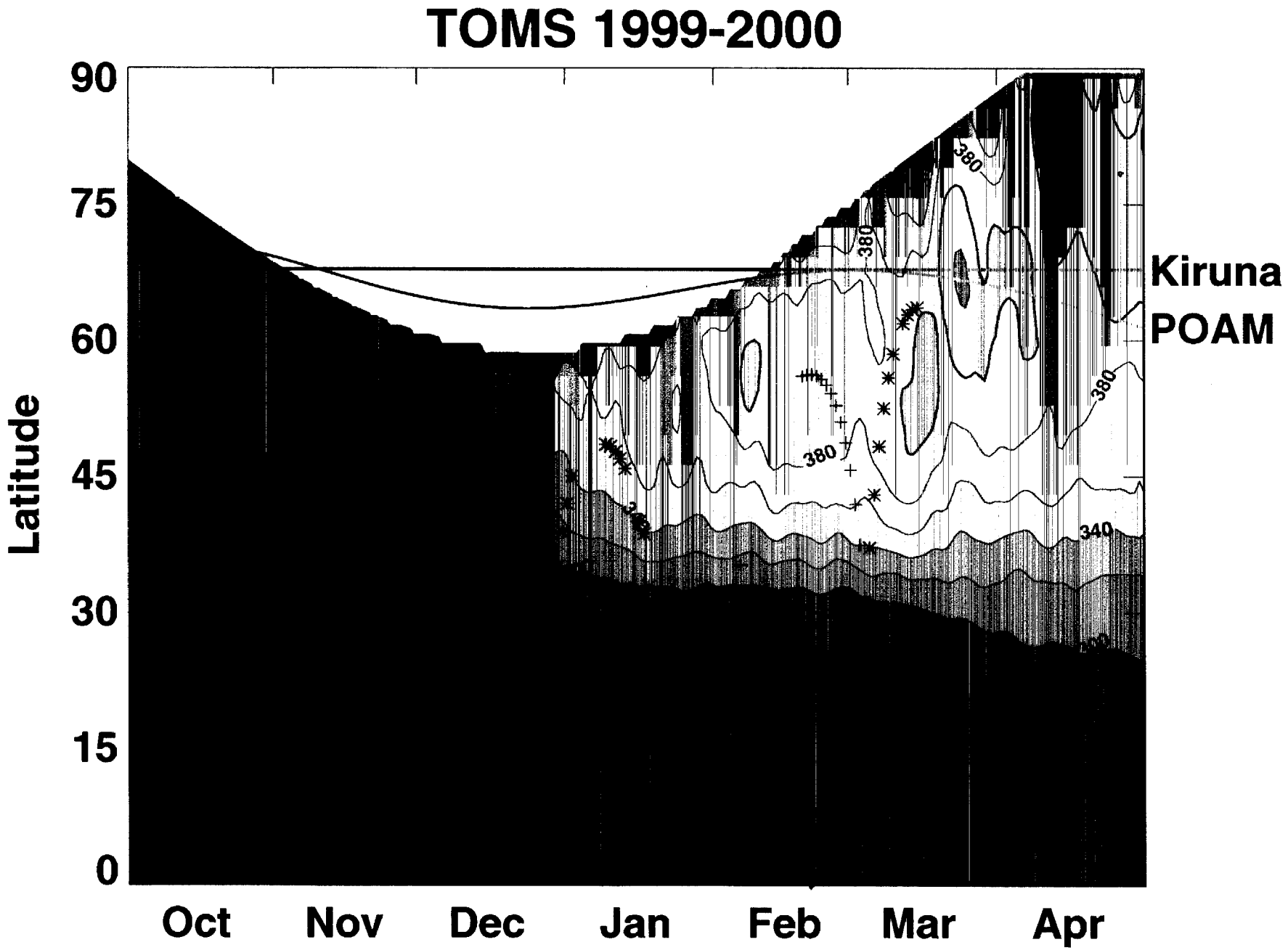
TOMS 1999-2000
90
75
60
45
30
15
0
Latitude
Oct
Nov
Dec
Jan
Feb
Mar
Apr
380
380
380
340
Kiruna
POAM

3

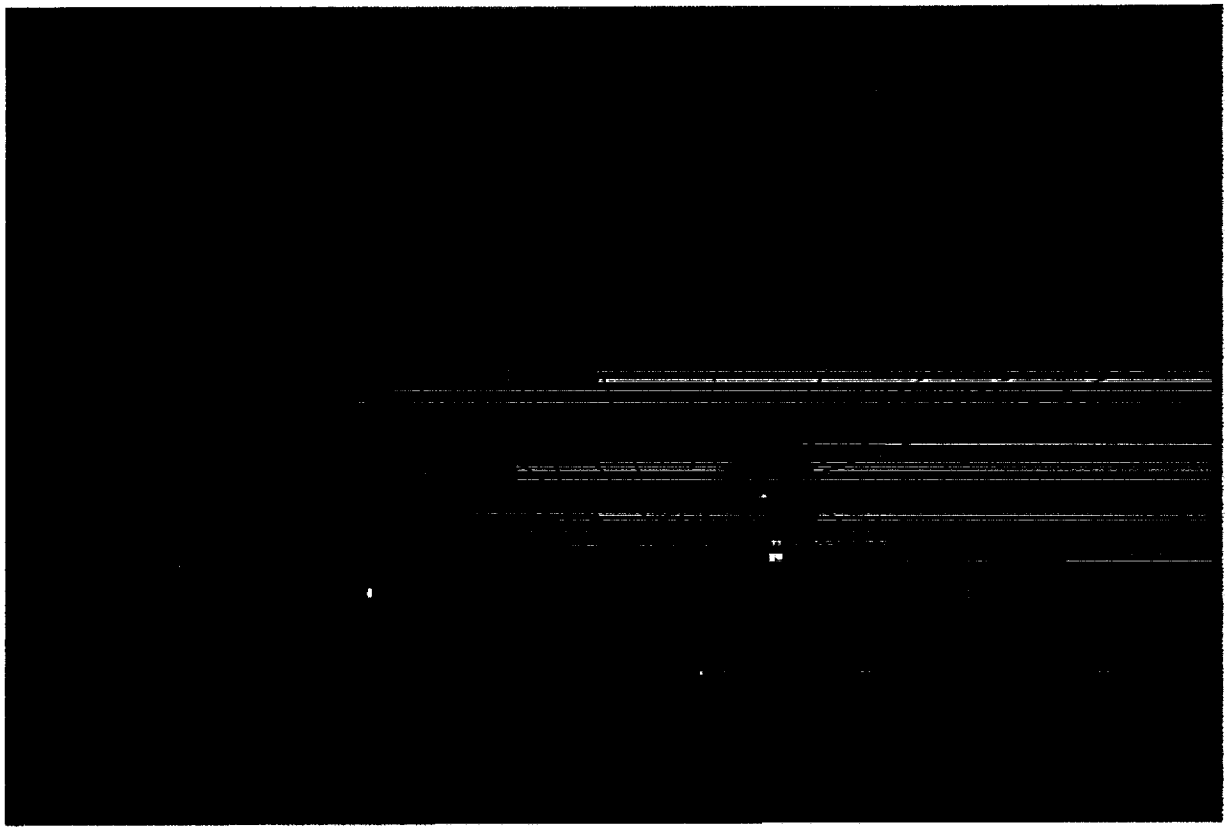

4

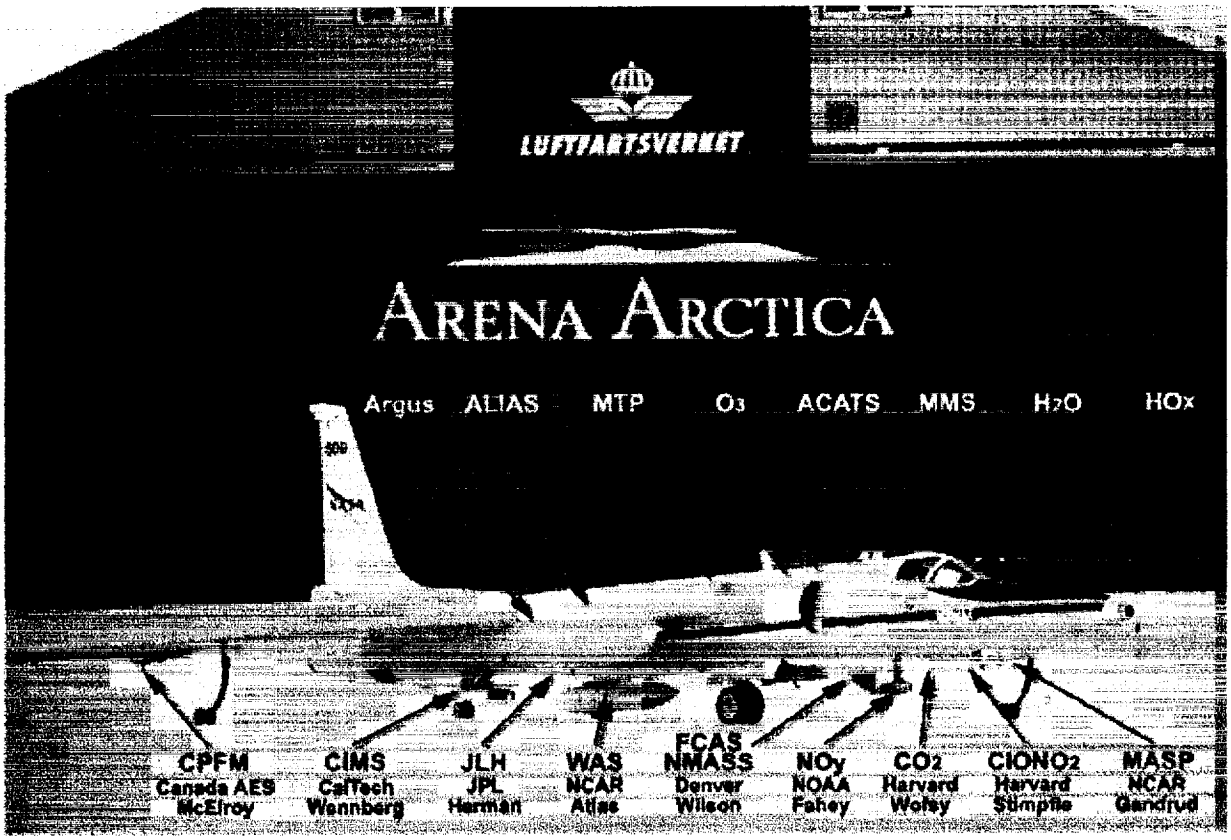
LUFTFARTSVERKET
ARENA ARCTICA
Argus
ALIAS
MTP
O3
ACATS
MMS
H2O
HOx
CPFM
Canada AES
McElroy
CIMS
CalTech
Wennberg
JLH
JPL
Herman
WAS
NCAR
Atlas
FCAS
NMASS
Denver
Wilson
NOy
NOAA
Fahey
CO2
Harvard
Wofsy
ClONO2
Harvard
Stimpfle
MASP
NCAR
Gandrud

OLEX

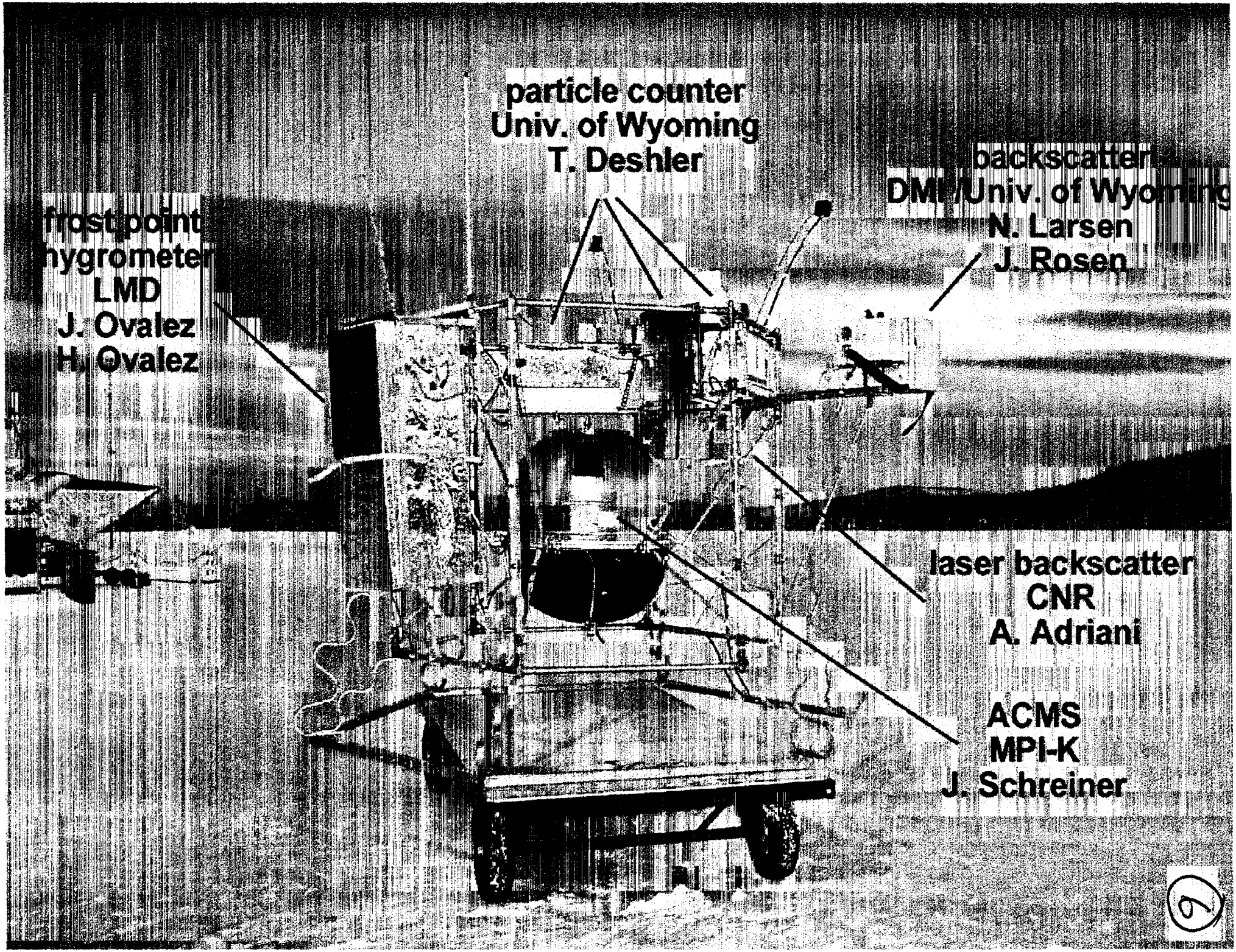
particle counter
Univ. of Wyoming
T. Deshler
backscatter
DMI/Univ. of Wyoming
N. Larsen
J. Rosen
frostpoint
hygrometer
LMD
J. Ovalez
H. Ovalez
laser backscatter
CNR
A. Adriani
ACMS
MPI-K
J. Schreiner

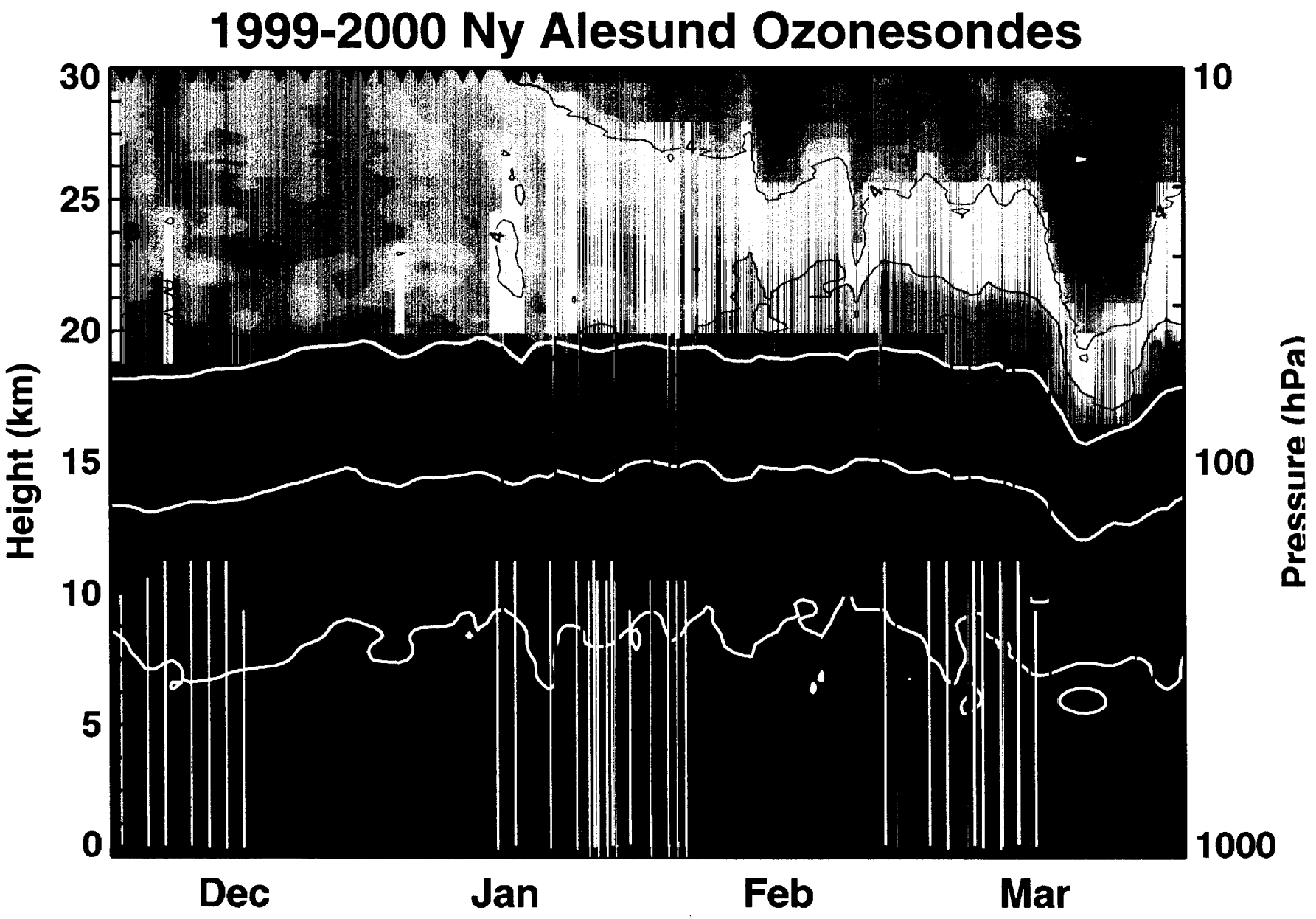
1999-2000 Ny Alesund Ozonesondes
Height (km)
30
25
20
15
10
5
0
Dec
Jan
Feb
Mar
10
100
1000
Pressure (hPa)

1999-2000 Vortex Temp. (K)

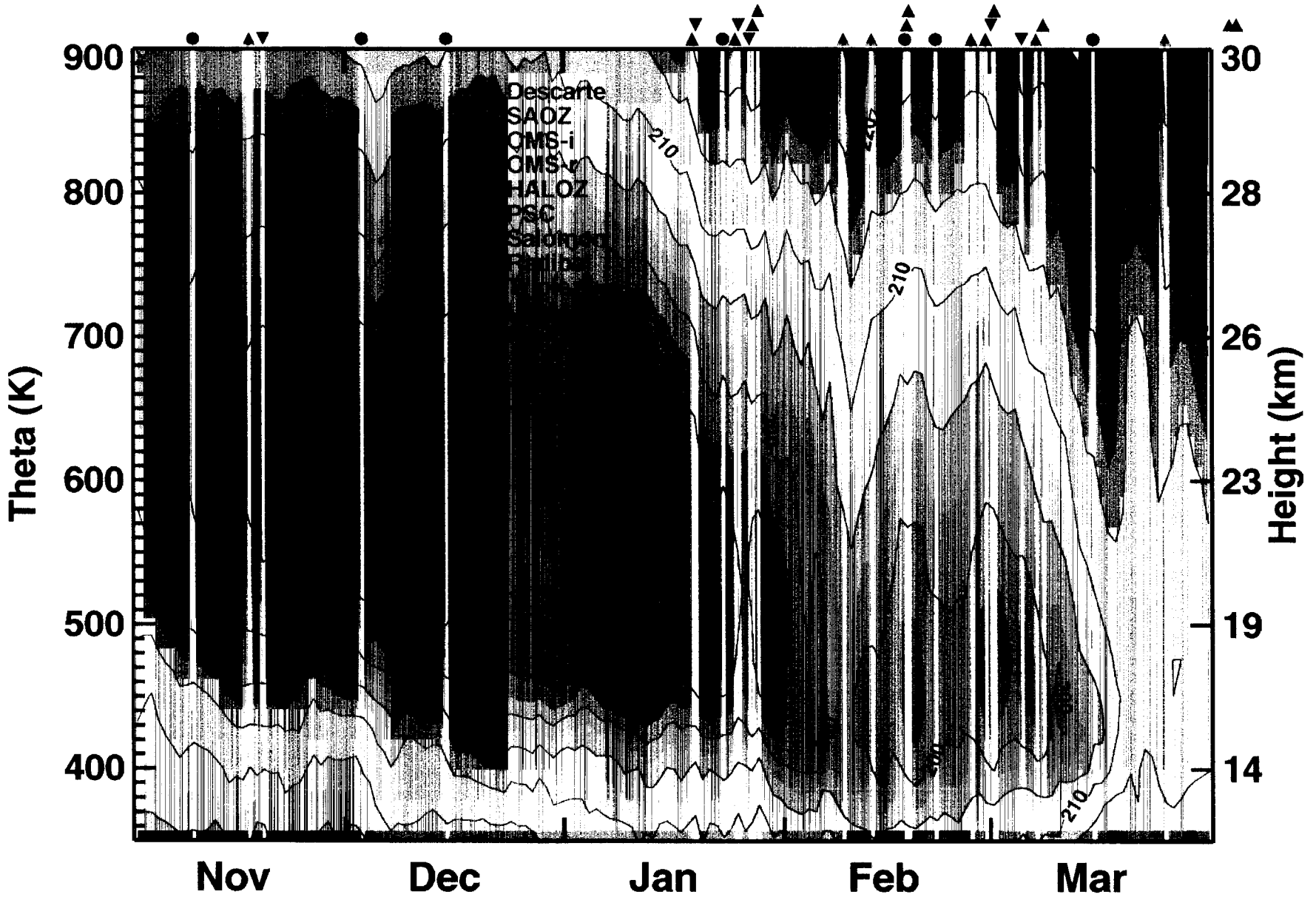

UKMO, Eql. 75-90°N

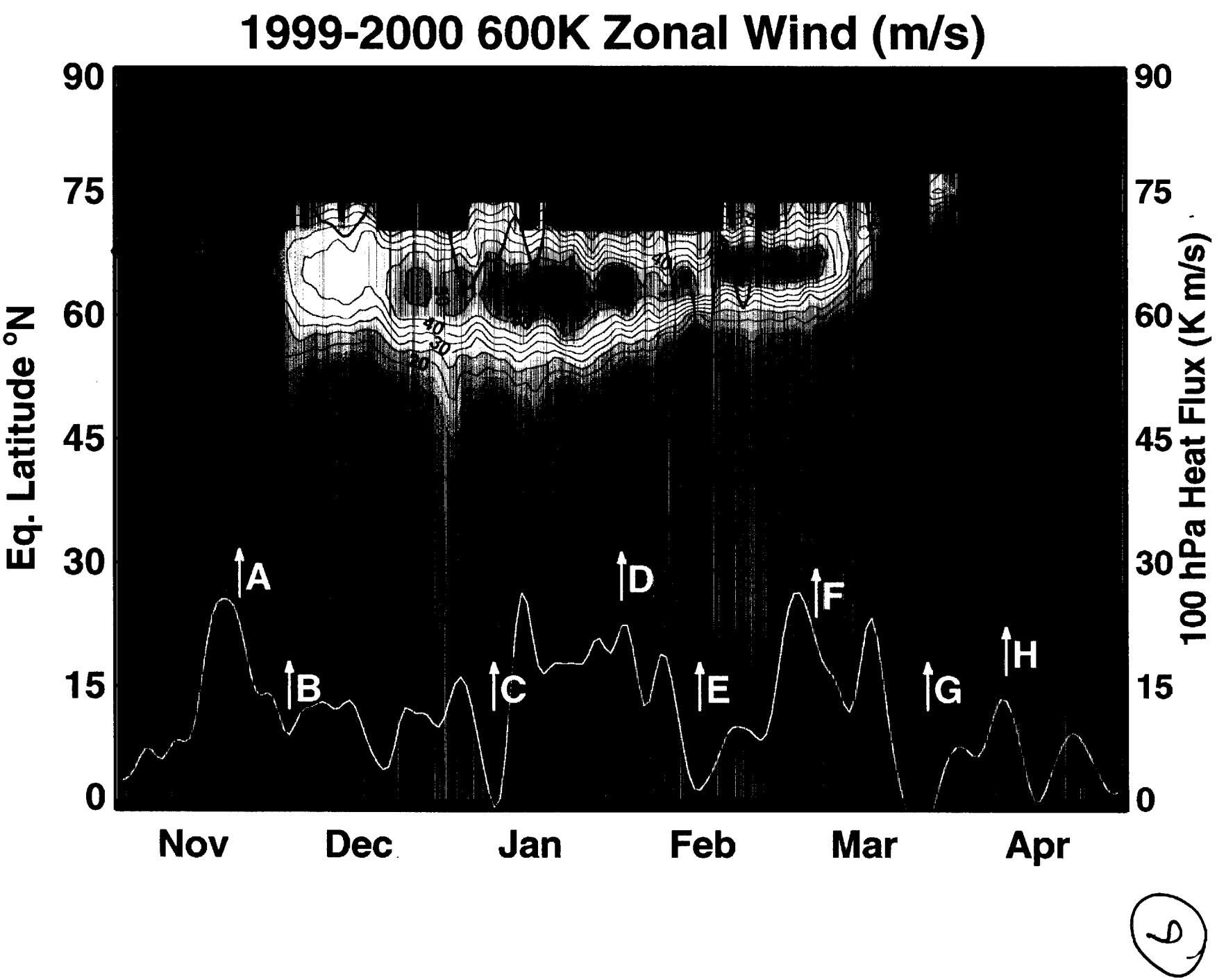
1999-2000 600K Zonal Wind (m/s)
Eq. Latitude °N
100 hPa Heat Flux (K m/s)
90
75
60
45
30
15
0
Nov
Dec
Jan
Feb
Mar
Apr
A
B
C
D
E
F
G
H
40
30
20

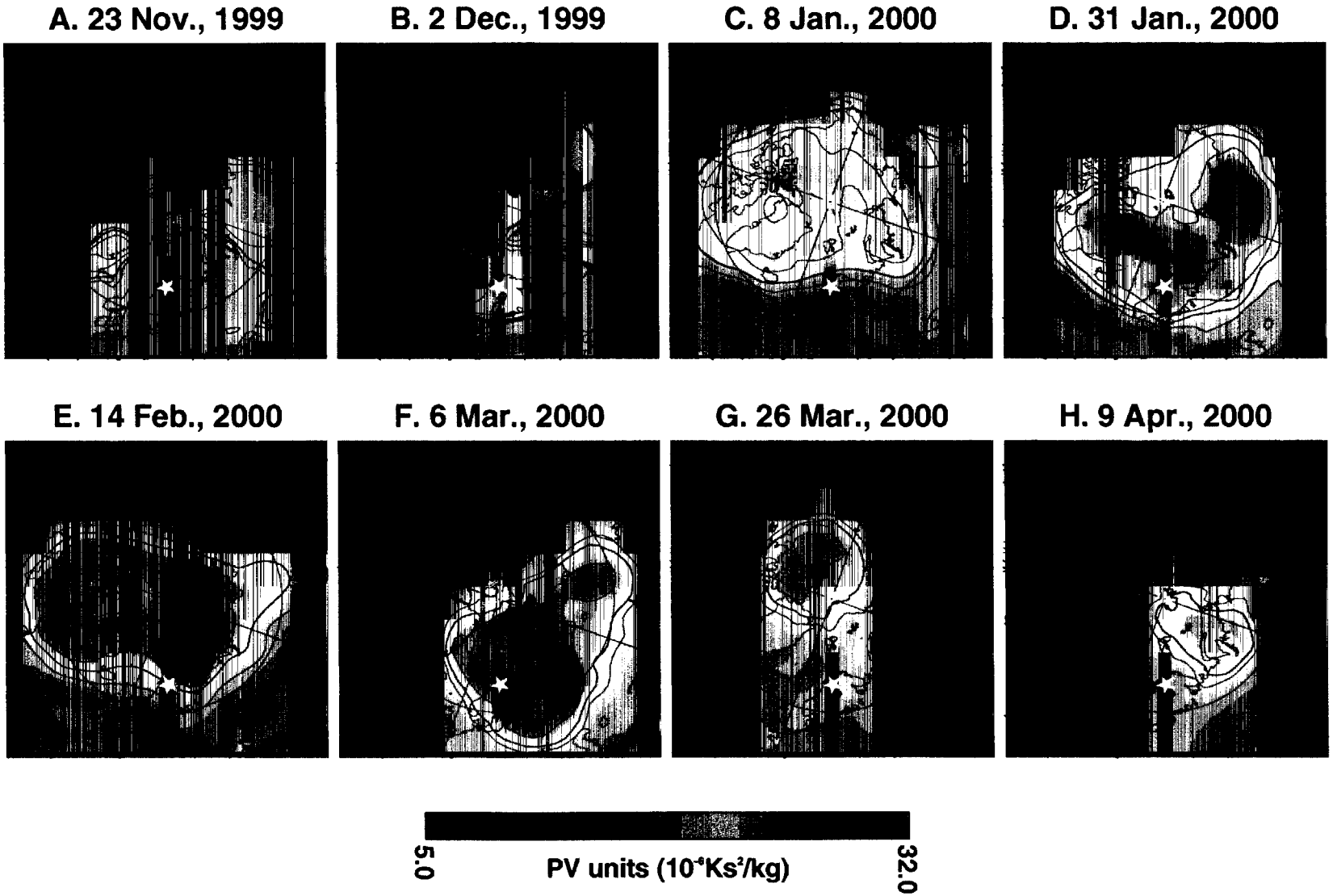
A. 23 Nov., 1999
B. 2 Dec., 1999
C. 8 Jan., 2000
D. 31 Jan., 2000
E. 14 Feb., 2000
F. 6 Mar., 2000
G. 26 Mar., 2000
H. 9 Apr., 2000
5.0
PV units (10⁻⁶Ks²/kg)
32.0

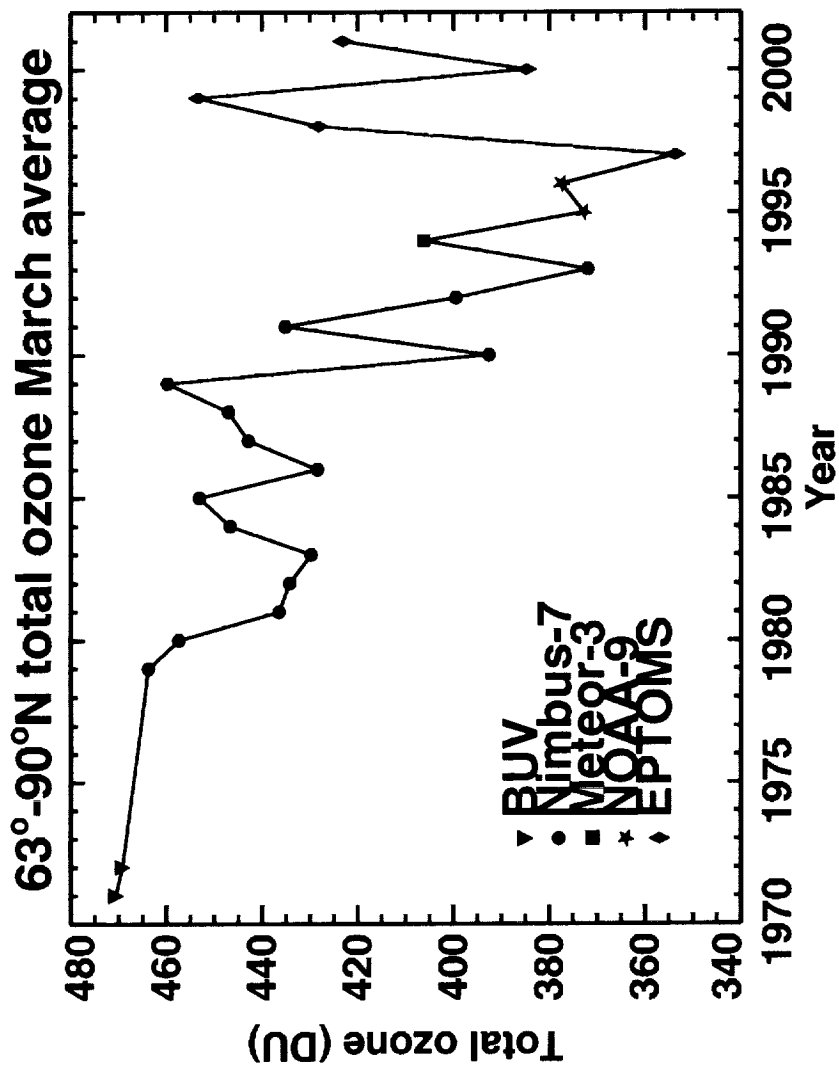
63°-90°N total ozone March average
Total ozone (DU)
480
460
440
420
400
380
360
340
1970
1975
1980
1985
1990
1995
2000
Year
BUV
Nimbus-7
Meteor-3
NOAA-9
EPTOMS